Dithio- and Diselenophosphinate Thorium(IV) and Uranium(IV) Complexes: Molecular and Electronic Structure, Spectroscopy, and Transmetalation Reactivity

Journal:	*Inorganic Chemistry*
Manuscript ID	ic-2015-01342d.R2
Manuscript Type:	Article
Date Submitted by the Author:	10-Nov-2015
Complete List of Authors:	Behrle, Andrew; University of Missouri, Chemistry Kerridge, Andrew; Lancaster University, Chemistry Walensky, Justin; University of Missouri, Columbia, Chemistry

Dithio- and Diselenophosphinate Thorium(IV) and Uranium(IV) Complexes: Molecular and Electronic Structure, Spectroscopy, and Transmetalation Reactivity

Andrew C. Behrle,[1] Andrew Kerridge,[2]* and Justin R. Walensky[1]*

[1] Department of Chemistry, University of Missouri, Columbia, MO 65211-7600

[2] Department of Chemistry, Lancaster University, Lancaster LA1 4YB, UK

Abstract

We report a comparison of the molecular and electronic structure of dithio- and diselenophosphinate, $(E_2PR_2)^{1-}$, E = S, Se; R = ^{i}Pr, ^{t}Bu, with thorium(IV) and uranium(IV) complexes. For the thorium dithiophosphinate complexes, reaction of $ThCl_4(DME)_2$ with four equivalents of KS_2PR_2 (R = ^{i}Pr, ^{t}Bu) produced the homoleptic complexes, $Th(S_2P^{i}Pr_2)_4$, **1S-Th-^{i}Pr**, and $Th(S_2P^{t}Bu_2)_4$, **, 2S-Th-^{t}Bu**. The diselenophosphinate complexes were synthesized in a similar manner using KSe_2PR_2 to produce $Th(Se_2P^{i}Pr_2)_4$, **1Se-Th-^{i}Pr**, and $Th(Se_2P^{t}Bu_2)_4$, **, 2Se-Th-^{t}Bu**. $U(S_2P^{i}Pr_2)_4$, **1S-U-^{i}Pr**, could be made directly from UCl_4 and four equivalents of $KS_2P^{i}Pr_2$. With $(Se_2P^{i}Pr_2)^{1-}$, using UCl_4 and three or four equivalents of $KSe_2P^{i}Pr_2$ yielded the mono-chloride product $U(Se_2P^{i}Pr_2)_3Cl$, **3Se-U^{iPr}-Cl**, but using $UI_4(1,4\text{-dioxane})_2$ produced the homoleptic $U(Se_2P^{i}Pr_2)_4$, **1Se-U-^{i}Pr**. Similarly, the reaction of UCl_4 with four equivalents of $KS_2P^{t}Bu_2$ yielded $U(S_2P^{t}Bu_2)_4$, **2S-U-^{t}Bu**, while the reaction with $KSe_2P^{t}Bu_2$ resulted in the formation of $U(Se_2P^{t}Bu_2)_3Cl$, **4Se-U^{tBu}-Cl**. Using $UI_4(1,4\text{-dioxane})_2$ and four equivalents of $KSe_2P^{t}Bu_2$ with UCl_4 in acetonitrile yielded $U(Se_2P^{t}Bu_2)_4$, **2Se-U-^{t}Bu**. Transmetalation reactions were investigated with complex **2Se-U-^{t}Bu** and various CuX (X = Br, I), salts to yield $U(Se_2P^{t}Bu_2)_3X$, (**6Se-U^{tBu}-Br,** and **7Se-U^{tBu}-I)** and 0.25 equivalents of $[Cu(Se_2P^{t}Bu_2)]_4$, **8Se-Cu-^{t}Bu**. Additionally **2Se-U-^{t}Bu** underwent transmetalation reactions with Hg_2F_2 and $ZnCl_2$ to yield $U(Se_2P^{t}Bu_2)_3F$, **6**, and $U(Se_2P^{t}Bu_2)_3Cl$, **4Se-U^{tBu}-Cl**, respectively. The molecular structures were analyzed using ^{1}H, ^{13}C, ^{31}P, and ^{77}Se NMR and IR spectroscopy and structurally

characterized using X-ray crystallography. Using the QTAIM approach, the electronic structure of all homoleptic complexes were probed and show slightly more covalent bonding character in actinide-selenium bonds over actinide-sulfur bonds.

Introduction

Recycling of spent nuclear fuel is important if nuclear energy is to be a viable source for a portion of the world's increasing energy requirements. In recent years, extractors bearing soft donor atoms have been shown to have selectivity for actinides over lanthanides.[1-3] In fact, Cyanex 301, a dithiophosphinic acid, is commercially used to extract late minor actinides from lanthanides.[4] This is presumed to be due to actinide-ligand bonding having more covalent character than lanthanides but further study is warranted. In this regard, the synthesis of dithio- and diselenophosphinate complexes with alkyl-substituents provides a platform from which to investigate this phenomenon.

The Gaunt group recently reported a series of 4f and 5f diphenyldiselenophosphinate complexes which showed enhanced covalent character in the actinide series than their lanthanide counterparts.[5] We followed with a comparison of sulfur- and selenium-based phosphonate compounds which observed actinide-selenium bonds had higher covalency than actinide-sulfur bonds.[6] For strongly oxophilic, Lewis acidic metal centers such as the actinides, this was an unexpected result and opens up new opportunities on how to describe actinide-ligand bonding.

The reactivity of actinide complexes with soft donor ligands is limited. Insertion of CO_2 and CS_2 into uranium-thiolato,[7,8] -sulfide, -selenide-, and telluride[9] bonds has been reported. In our previous work we noted that insertion reactivity was not observed with dithio- and diselenophosphonate complexes but realized this could be due to steric crowding around the metal center. Given our interest in coinage metal chemistry,[10] which have a propensity for soft

donor atoms such as sulfur and selenium, transmetalation reactions with soft metal salts seemed plausible. These reactions are advantageous to achieve stoichiometric substitution at one site on the actinide and hence examine structure, bonding, and spectroscopic differences. Herein, we report the synthesis of $An(E_2PR_2)_4$ (An = Th, U; E = S, Se; R = ^{i}Pr, ^{t}Bu) complexes and transmetalation reactions with $U(Se_2P^tBu_2)_4$ and CuBr, CuI, $ZnCl_2$, and Hg_2F_2 salts to produce compounds of the form $XU(Se_2P^tBu_2)_3$.

Experimental

General considerations. The syntheses and manipulations described below were conducted using standard Schlenk and glovebox techniques. All reactions were conducted in a Vacuum Atmospheres inert atmosphere (N_2) glovebox. THF, toluene, and hexanes were purchased anhydrous, stored over activated 4 Å molecular sieves, and sparged with nitrogen prior to use. Methylene chloride and ethanol (200 proof) were dried over activated 4 Å molecular sieves and sparged with nitrogen for thirty minutes prior to use. $[ThCl_4(DME)_2]$,[11] and $[UCl_4]$[12] were synthesized as previously described. $[Th(S_2P^iPr_2)_4]$[13] and $[KS_2P^iPr_2]$,[14] were synthesized using modified literature procedures (*vide infra*). Diisopropylphosphine (10% in hexanes), di-*tert*-butylphosphine, sublimed sulfur, selenium, potassium hydroxide, $[Cu(NCMe)_4]PF_6$, copper(I) chloride, Hg_2F_2, $HgCl_2$, copper(I) bromide, and copper(I) iodide were purchased from commercial suppliers and used without further purification. Benzene-d_6 and THF-d_8 (Cambridge Isotope Laboratories) were dried over molecular sieves and degassed with three freeze-evacuate-thaw cycles. D_2O (Cambridge Isotope Laboratories) was used as received. All ^{1}H, ^{13}C, ^{31}P, and ^{77}Se NMR data were obtained on a 300 MHz DRX or 500 MHz DRX Bruker spectrometer. ^{1}H NMR shifts given were referenced internally to the residual solvent peaks at δ 7.16 ppm (C_6D_5H), δ 1.72 ppm (C_4D_7HO), δ 4.79 (HDO). ^{13}C NMR shifts given were referenced internally

to the residual peaks at δ 128.0 ppm (C_6D_6) or δ 67.20 (C_4D_8O). ^{31}P NMR spectra were externally referenced to 0.00 ppm with 5% H_3PO_4 in D_2O. ^{77}Se NMR shifts given were referenced externally to 460.00 ppm with diphenyl diselenide in C_6D_6, C_4D_8O, or D_2O. Infrared spectra were recorded as KBr pellets on Perkin-Elmer Spectrum One FT-IR spectrometer. Elemental analyses were performed by Atlantic Microlab, Inc. (Norcross, GA).

Crystallographic Data Collection and Structure Determination. The selected single crystal was mounted on nylon cryoloops using viscous hydrocarbon oil. X-ray data collection was performed at 173(2) or 100(2) K. The X-ray data were collected on a Bruker CCD diffractometer with monochromated Mo-Kα radiation (λ = 0.71073 Å) or Cu- Kα radiation (λ = 1.54178 Å). The data collection and processing utilized Bruker Apex2 suite of programs.[15] The structures were solved using direct methods and refined by full-matrix least-squares methods on F2 using Bruker SHELX-2014/7 program.[16] All non-hydrogen atoms were refined with anisotropic displacement parameters. All hydrogen atoms were placed at calculated positions and included in the refinement using a riding model. Thermal ellipsoid plots were prepared by using X-seed[17] with 50% of probability displacements for non-hydrogen atoms. Crystal data and details for data collection for complexes **1-5**, **7-10**, **13**, and **15** are provided in Tables 1 and 2. Significant bond distances and angles are listed in Tables 5-9 and 10.

$KS_2P^iPr_2$. An oven-dried 100 mL Schlenk flask was charged with diisopropylphosphine (10 g, 8.46 mmol) and cycled onto a Schlenk line. 30 mL of 200 proof ethanol was added to diisopropylphosphine followed by potassium hydroxide (475 mg, 8.46 mmol) and elemental sulfur (543 mg, 2.12 mmol). The reaction was allowed to stir at room temperature for 12 h to yield a colorless solution. The ethanol was removed under vacuum to yield a white precipitate and the Schlenk flask was taken inside the glove box. The white precipitate was washed twice

with 20 mL of diethyl ether, filtered over a frit, and dried to yield a white powder (1.77 g, 95%). ^{1}H NMR (D_2O, 25 °C): δ 2.22-2.16 (m, 2H, C*H*(CH_3)), 1.18 (dd, $^{3}J_{P\text{-}H}$ = 18.0 Hz, $^{3}J_{H\text{-}H}$ = 7.0 Hz, 12H, CH(C*H*$_3$)). ^{13}C{^{1}H} (D_2O, 25 °C, uncorrected): δ 33.03 (d, $^{1}J_{P\text{-}C}$ = 50.3 Hz), 15.74. ^{31}P{^{1}H} (D_2O, 25 °C): δ 95.6. IR (cm^{-1}): 2982 (s), 2870 (s), 1479 (m), 1388 (m), 1365 (m), 1177 (s), 1124 (s), 1110 (s), 1025 (s), 804 (m), 625 (s), 612 (s), 520 (m), 473 (m).

$KS_2P^tBu_2$. An oven-dried 120 mL Schlenk flask was charged with $^{t}Bu_2PH$ (1.0 g, 6.84 mmol) followed by THF (3 mL). The Schlenk flask was cycled onto the Schlenk line and 20 mL of 200 proof ethanol was added followed by potassium hydroxide (384 mg, 6.84 mmol). The mixture was stirred until the potassium hydroxide was dissolved followed by addition of element sulfur (439 mg, 1.71 mmol). The reaction was stirred until the sulfur was consumed. The solvent was removed under vacuum to yield a white solid which was triturated with 20 mL of hexanes to yield a white microcrystalline powder (1.46 g, 86%). ^{1}H NMR (D_2O, 25 °C): δ 1.37 (d, $^{3}J_{P\text{-}H}$ = 16 Hz, 18 H, C(C*H*$_3$)$_3$). ^{13}C{^{1}H} (D_2O, 25 °C, uncorrected): δ 40.97 (d, $^{1}J_{P\text{-}C}$ = 41 Hz), 27.40 (d, $^{2}J_{P\text{-}C}$ = 2.0 Hz). ^{31}P{^{1}H} (D_2O, 25 °C): δ 112.4. IR (cm^{-1}): 2963 (s), 2891 (s), 1473 (m), 1383 (m), 1358 (m), 1173 (s), 1127 (s), 1108 (s), 1016 (s), 806 (m), 629 (s), 609 (s), 517 (m), 469 (m).

$KSe_2P^iPr_2$. Following the same procedure for $KS_2P^iPr_2$, diisopropylphosphine (10 g, 8.46 mmol), potassium hydroxide (475 mg, 8.46 mmol), and elemental selenium (1.34 g, 17.0 mmol) to yield a white powder (2.65 g, 99%). ^{1}H NMR (D_2O, 25 °C): δ 2.26-2.20 (m, 2H, C*H*(CH_3)), 1.18 (dd, $^{3}J_{P\text{-}H}$ = 20.0 Hz, $^{3}J_{H\text{-}H}$ = 7.0 Hz, 12H, CH(C*H*$_3$)). ^{13}C{^{1}H} (D_2O, 25 °C, uncorrected): δ 32.93 (d, $^{1}J_{P\text{-}C}$ = 36.0 Hz), 16.58 (d, $^{2}J_{P\text{-}C}$ = 13.0 Hz). ^{31}P{^{1}H} (D_2O, 25 °C): δ 70.1 (s + d satellites, $^{1}J_{Se\text{-}P}$ = 553.0 Hz). ^{77}Se{^{1}H} (D_2O, 25 °C): δ −192.01 (d, $^{1}J_{P\text{-}Se}$ = 553 Hz). IR (cm^{-1}): 2970 (s), 2913 (s), 2862 (s), 1459 (s), 1379 (s), 1291 (m), 1236 (m), 1160 (w), 1100 (m), 1083 (w), 1021 (s), 965 (w), 929 (w), 883 (s), 837 (w), 655 (s), 593 (s).

$KSe_2P^tBu_2$. A 120 mL Schlenk flask was charged with $^tBu_2PH$ (1.0 g, 6.84 mmol) and THF (3mL). The flask was cycled onto a Schlenk line and 20 mL of 200 proof ethanol was added followed by potassium hydroxide (384 mg, 6.84 mmol). The mixture was stirred until the potassium hydroxide was dissolved followed by addition of elemental selenium (1.08 g, 13.7 mmol). The reaction was stirred overnight and filtered via cannula. The solvent was removed under vacuum to yield a yellow solid which was washed with 20 mL of hexanes, filtered over a frit, and dried under vacuum to yield a white microcrystalline powder (1.74 g, 74%). ^{1}H NMR (D_2O, 25 °C): δ 1.42 (d, $^3J_{P\text{-}H}$ = 17.0 Hz, 18 H, C(CH_3)$_3$). $^{13}C\{^1H\}$ (D_2O, 25 °C, uncorrected): δ 40.27 (d,$^1J_{P\text{-}C}$ = 25 Hz), 27.79 (d, $^2J_{P\text{-}C}$ = 2.5 Hz). $^{31}P\{^1H\}$ (D_2O, 25 °C): δ 95.7 (s + d satellites, $^1J_{Se\text{-}P}$ = 556 Hz). $^{77}Se\{^1H\}$ (D_2O, 25 °C): δ −153.5 (d, $^1J_{P\text{-}Se}$ = 556 Hz). IR (cm^{-1}): 2962 (m), 2911 (m), 1459 (m), 1382 (m), 1357 (m), 1170 (s), 1088 (s), 1019 (s), 803 (m), 599 (w), 578 (w), 537 (s), 484 (m).

$Th(S_2P^iPr_2)_4$, 1S-Th-^{i}Pr. A 20 mL scintillation vial was charged with $ThCl_4(DME)_2$ (174 mg, 0.314 mmol) and THF (3 mL). A second 20 mL scintillation vial was charged with $KS_2P^iPr_2$ (283 mg, 1.28 mmol) and THF (3 mL). The solution of $KS_2P^iPr_2$ was added to a stirring solution of $ThCl_4(DME)_2$ and allowed to stir for 14 h at room temperature. The reaction solvent was removed under vacuum and the precipitate was extracted twice with toluene, filtered over a bed of Celite, concentrated, and layered with Et_2O to yield a white microcrystalline material (180 mg, 60%). Colorless X-ray quality crystals were grown from a concentrated Tol/Et_2O mixture at −20 ºC. ^{1}H NMR (C_6D_6, 25 °C): δ 2.36 (d sep, $^2J_{P\text{-}H}$ = 10.0 Hz, $^3J_{H\text{-}H}$ = 7.5 Hz, 8H, CH(CH_3)$_2$), 1.23 (dd, $^3J_{P\text{-}H}$ = 20.0 Hz, $^3J_{H\text{-}H}$ = 7.5 Hz, CH(CH_3)$_2$). $^{13}C\{^1H\}$ (C_6D_6, 25 °C): δ 35.19 (d, $^1J_{P\text{-}C}$ = 43.0 Hz), 17.00. $^{31}P\{^1H\}$ (C_6D_6, 25 °C): δ 84.9. IR (cm^{-1}): 2960 (s), 2925 (s), 2860 (s), 2427 (w), 1460 (s), 1387 (s), 1288 (m), 1245 (m), 1160 (w), 1090 (m), 1048 (m), 1026 (m), 930 (m), 881

(s), 838 (w), 690 (m), 671 (s), 632 (s), 500 (s). Anal. calcd. for $C_{24}H_{56}P_4S_8Th$: C, 30.12%; H, 5.90%. Found C, 29.90%; H, 5.66%.

$Th(S_2P^tBu_2)_4$, 2S-Th-^{t}Bu. A 20 mL scintillation vial was charged with $ThCl_4(DME)_2$ (109 mg, 0.196 mmol) and THF (3 mL). A second 20 mL scintillation vial was charged with $KS_2P^tBu_2$ (200 mg, 0.805 mmol) and THF (3 mL). The $KS_2P^tBu_2$ was added to a stirring solution of $ThCl_4(DME)_2$ and allowed to stir for 14 h at room temperature. The solvent removed under vacuum, extracted with toluene, and filtered over Celite. The toluene was removed under vacuum to yield a pale yellow residue which was extracted with THF, filtered over Celite and concentrated to yield a white microcrystalline solid (84 mg, 42%). X-ray quality crystals were grown from a concentrated THF/hexanes mixture at room temperature. ^{1}H NMR (C_6D_6, 25 °C): δ 1.43 (d, $^3J_{P\text{-}H}$ = 15.0 Hz, 72 H, C(CH_3)$_3$). ^{13}C{^{1}H} (C_6D_6, 25 °C): δ 42.97 (d, $^1J_{P\text{-}C}$ = 34.0 Hz), 27.44. ^{31}P{^{1}H} (C_6D_6, 25 °C): δ 99.1. IR (cm^{-1}): 2990 (m), 2964 (m), 2904 (m), 2868 (m), 1475 (s), 1390 (m), 1364 (m), 1181 (s), 1082 (s), 1088 (s), 939 (m), 804 (m), 620 (s), 518 (m), 467 (m), 441 (m). Anal. calcd. for $C_{32}H_{72}P_4S_8Th$•0.5(THF): C, 36.94%; H, 6.93%. Found C, 36.99%; H, 6.87%.

$Th(Se_2P^iPr_2)_4$, 1Se-Th-^{i}Pr. A 20 mL scintillation vial was charged with $ThCl_4(DME)_2$ (97 mg, 0.175 mmol) and THF (3 mL) A second 20 mL scintillation vial was charged with $KSe_2P^iPr_2$ (225 mg, 0.716 mmol) and THF (3 mL). Both vials were placed inside a −20 ºC freezer for 10 min. The solution of $KSe_2P^iPr_2$ was added to a stirring solution of $ThCl_4(DME)_2$ and allowed to stir at room temperature for 14 h resulting in a yellow solution. The reaction solvent was removed under vacuum and the precipitate was extracted twice with toluene, filtered over a bed a Celite, and the solvent removed under reduced pressure to yield a white precipitate (182 mg, 78%). Colorless X-ray quality crystals were grown from concentrated Tol/Et_2O mixture at -23

°C. ^{1}H NMR (C_6D_6, 25 °C): δ 2.41-2.39 (m, 8H, C*H*(CH_3)$_2$), 1.25 (dd, $^{3}J_{P\text{-}H}$ = 20.0 Hz, $^{3}J_{H\text{-}H}$ = 7.0 Hz, 48H, CH(C*H*$_3$)$_2$). ^{13}C{^{1}H} (C_6D_6, 25 °C): δ 34.12 (d, $^{1}J_{P\text{-}C}$ = 29.0 Hz), 17.69. ^{31}P{^{1}H} (C_6D_6, 25 °C): δ 57.6 (s + d satellites, $^{1}J_{Se\text{-}P}$ = 500 Hz). ^{77}Se{^{1}H} (C_6D_6, 25 °C): δ 6.4 (d, $^{1}J_{P\text{-}Se}$ = 500 Hz). IR (cm^{-1}): 2960 (s), 2925 (m), 2867 (m), 1459 (s), 1384 (s), 1237 (m), 1159 (w), 1091 (w), 1047 (w), 1023 (w), 930 (w), 878 (m), 837 (w), 649 (s), 615 (m), 538 (s). 478 (m). Anal. calcd. for $C_{24}H_{56}P_4Se_8Th$: C, 21.64%; H, 4.24%. Found C, 21.82%; H, 4.13%.

Th(Se$_2$P^{t}Bu$_2$)$_4$, 2Se-Th-^{t}Bu. A 20 mL scintillation vial was charged with $ThCl_4(DME)_2$ (77 mg, 0.138 mmol) and THF (3 mL). A second 20 mL scintillation vial was charged with $KSe_2P^tBu_2$ (194 mg, 0.567 mmol) and THF (3 mL). The $KSe_2P^tBu_2$ was added to a stirring solution of $ThCl_4(DME)_2$ and allowed to stir for 14 h at room temperature. The solvent removed under vacuum, extracted with toluene, and filtered over Celite. The toluene was removed under vacuum to yield a pale yellow residue which was extracted with THF, filtered over Celite and concentrated to yield a white microcrystalline solid (122 mg, 61%). X-ray quality crystals were grown from a concentrated THF/hexanes mixture at room temperature. ^{1}H NMR (C_6D_6, 25 °C): δ 1.45 (d, $^{3}J_{P\text{-}H}$ = 17.0 Hz, 72H, C(C*H*$_3$)$_3$). ^{13}C{^{1}H} (C_6D_6, 25 °C): δ 42.21 (d, $^{1}J_{P\text{-}C}$ = 18.0 Hz), 28.29. ^{31}P{^{1}H} (C_6D_6, 25 °C): δ 78.3 (s + d satellites, $^{1}J_{Se\text{-}P}$ = 491 Hz). ^{77}Se{^{1}H} (C_6D_6, 25 °C): δ 90.5 (d, $^{1}J_{P\text{-}Se}$ = 491 Hz). IR (cm^{-1}): 2984 (s), 2950 (s), 2913 (s), 2860 (s), 1473 (s), 1389 (m), 1364 (s), 1261 (w), 1175 (s), 1096 (m), 1071 (m), 1021 (m), 938 (w), 802 (m), 583 (s), 534 (s), 483 (s). Anal. calcd. for $C_{32}H_{72}P_4Se_8Th{\bullet}C_4H_8O$: C, 28.51%; H, 5.32%. Found C, 28.74%; H, 5.09%.

U(S$_2$P^{i}Pr$_2$)$_4$, 1S-U-^{i}Pr. A 20 mL scintillation vial was charged with UCl_4 (99 mg, 0.261 mmol) and THF (3 mL). A second 20 mL scintillation vial was charged with $KS_2P^iPr_2$ (235 mg, 1.07 mmol) and THF (3 mL). Both vials were placed in a freezer at −20 ºC for 10 min. The $KS_2P^iPr_2$

was added to a stirring solution of UCl_4 and underwent a color change to green. The reaction was allowed to warm to room temperature and stirred for 5 h. The solvent was removed under reduced pressure and the solid was extracted with toluene, filtered over Celite, concentrated and layered with diethyl ether. Green X-ray quality crystals were grown at room temperature (158 mg, 63%).^{1}H NMR (C_6D_6, 25 °C): δ 8.00 (s, br, 8H, C*H*(CH_3)$_2$), 4.20 (s, br, 48H, CH(C*H*$_3$)$_2$). ^{31}P{^{1}H} (C_6D_6, 25 °C): δ −436.3. IR (cm^{-1}): 2962 (s), 2927 (m), 2869 (m), 1458 (s), 1384 (s), 1244 (m), 1151 (w), 1088 (m), 1048 (m), 1025 (m), 941 (w), 879 (s), 838 (m), 724 (w), 673 (s), 646 (s), 505 (m). Anal. calcd. for $C_{24}H_{56}P_4S_8U$: C, 29.93%; H, 5.86%. Found C, 30.25%; H, 5.81%.

U($S_2P^tBu_2$)$_4$, 2S-U-^{t}Bu. A 20 mL scintillation vial was charged with UCl_4 (88 mg, 0.232 mmol) and THF (3 mL). A second 20 mL scintillation vial was charged with $KS_2P^tBu_2$ (237 mg, 0.954 mmol) and THF (4 mL) and placed in a freezer at −20 ºC for 20 min. The $KS_2P^tBu_2$ was added to a stirring solution of UCl_4 and resulted in a green/yellow color change. The reaction mixture was allowed to warm to room temperature and stirred for 17 h. The solvent was removed under vacuum, extracted with toluene, filtered over a bed of Celite, and solvent removed to yield a yellow precipitate (134 mg, 54%). ^{1}H NMR (C_6D_6, 25 °C): δ −11.90. (s, br, 72H, C(C*H*$_3$)$_3$). ^{31}P{^{1}H} (C_6D_6, 25 °C): δ −467.2. IR (cm^{-1}): 2988 (m), 2965 (m), 2900 (m), 2873 (m), 1473 (s), 1393 (m), 1360 (m), 1180 (s), 1089 (s), 1082 (s), 939 (m), 804 (m), 621 (s), 518 (m), 466 (m). Anal. calcd. for $C_{32}H_{72}P_4S_8U$: C, 35.74%; H, 6.75%. Found C, 35.90%; H, 6.82%.

U($Se_2P^iPr_2$)$_4$, 1Se-U-^{i}Pr. A 20 mL scintillation vial was charged with UI_4(1,4-dioxane)$_2$ (138 mg, 0.150) mmol). A second 20 mL scintillation vial was charged with $KSe_2P^iPr_2$ (192 mg, 0.611 mmol) and acetonitrile (4 mL). The solution of $KSe_2P^iPr_2$ was placed in a freezer at −20 °C for 20 min. The UI_4(1,4-dioxane)$_2$ was added as a solid to a stirring solution of $KSe_2P^iPr_2$ and

resulted in a red color change. The reaction mixture was allowed to stir at room temperature for 5 h, filtered over Celite, and the solvent removed under vacuum to yield a red precipitate. The precipitate was extracted with diethyl ether, filtered over Celite, and the solvent reduced to yield a red precipitate (109 mg, 55%). X-ray quality crystals were grown from a concentrated diethyl ether solution at room temperature. ^{1}H NMR (C_6D_6, 25 °C): δ 7.34 (s, br, 8H, C*H*(CH_3)$_2$), 4.37 (s, br, 48H, CH(C*H*$_3$)$_2$). ^{31}P{^{1}H} (C_6D_6, 25 °C): δ −618.0 (s + d satellites, $^{1}J_{Se\text{-}P}$ = 497 Hz). IR (cm^{-1}): 2959 (s), 2919 (s), 2867 (s) 1467 (s), 1382 (m), 1359 (m), 1234 (m), 1156 (m), 1087 (m), 1038 (m), 1018 (m), 920 (w), 875 (m), 645 (m), 613 (s), 538 (s), 469 (w). Anal. calcd. for $C_{24}H_{56}P_4Se_8U$: C, 21.54%; H, 4.22%. Found C, 21.91%; H, 4.08%.

U(Se$_2$P^{t}Bu$_2$)$_4$, 2Se-U-^{t}Bu. A 20 mL scintillation vial was charged with UCl_4 (65 mg, 0.171 mmol) and acetonitrile (2 mL). A second 20 mL scintillation vial was charged with $KSe_2P^tBu_2$ (241 mg, 0.704 mmol) and acetonitrile (3 mL). Both vials were placed in −20 ºC freezer for 20 min. The $KSe_2P^tBu_2$ was added to the UCl_4 and the reaction mixture was allowed to stir for 3 h. The reaction mixture was centrifuged and the orange precipitate was dried, extracted with toluene, and filtered over Celite to yield a red solution. X-ray quality crystals were grown from a concentrated toluene solution at −20 ºC (198 mg, 80%). ^{1}H NMR (C_6D_6, 25 °C): δ 2.74 (d, $^{3}J_{P\text{-}H}$ = 9.0 Hz, 72H, C(C*H*$_3$)$_3$). ^{31}P{^{1}H} (C_6D_6, 25 °C): δ −473.0. IR (cm^{-1}): 2961 (m), 2936 (m), 2900 (m), 2859 (m), 1470 (m), 1388 (m), 1362 (m), 1173 (m), 1095 (m), 1070 (m), 1020 (m), 929 (m), $_8$81 (m), 586 (m), 566 (s), 536 (m), 484 (m). Anal. calcd. for $C_{32}H_{72}P_4Se_8U$•(C_7H_8): C, 30.36%; H, 5.23%. Found C, 30.63%; H, 5.23%.

U(Se$_2$P^{i}Pr$_2$)$_3$Cl, 3Se-U^{iPr}-Cl. A 20 mL scintillation vial was charged with UCl_4 (152 mg, 0.400 mmol) and THF (2 mL). A second 20 mL scintillation vial was charged with $KSe_2P^iPr_2$ (390 mg, 1.24 mmol) and THF (3 mL). Both vials were placed in −23 °C freezer for 10 min and $KSe_2P^iPr_2$

was added to UCl_4 with an immediate color change to dark red. The reaction was allowed to stir for 5 h. The solvent was removed under vacuum and the red precipitate was extracted with toluene, filtered over a bed of Celite, and concentrated to yield a red microcrystalline solid (352 mg, 80%). X-ray quality crystals were grown from a concentrated diethyl ether solution at −23 °C. ^{1}H NMR (C_6D_6, 25 °C): δ 7.33 (s, br, 6H, C*H*(CH_3)$_2$), 4.36 (s, br, 36H, CH(C*H*$_3$)$_2$). ^{31}P{^{1}H} (C_6D_6, 25 °C): δ −610.2 (s + d satellites, $^1J_{Se\text{-}P}$ = 487 Hz). IR (cm^{-1}): 2959 (s), 2925 (m), 2866 (m), 1459 (s), 1387 (s), 1236 (m), 1158 (w), 1090 (m), 1047 (m), 1023 (m), 925 (w), 878 (m), 837 (w), 649 (s), 615 (s), 535 (s), 473 (m). Anal. calcd. for $C_{18}H_{42}ClP_3Se_6U$•0.5(Et_2O)•0.5(C_7H_8): C, 21.07%; H, 3.84%. Found C, 21.38%; H, 3.85%.

U(S$_2$P^{t}Bu$_2$)$_3$Cl, 4S-U^{tBu}-Cl. *Method A*. A 20 mL scintillation vial was charged with UCl_4 (76 mg, 0.200 mmol) and CH_3CN (3 mL). A second 20 mL scintillation vial was charged with $KS_2P^tBu_2$ (154 mg, 0.620 mmol) and CH_3CN (3 mL). Both vials were placed in a −23 °C freezer for 30 min and the $KS_2P^tBu_2$ was added to the UCl_4 mixture and allowed to stir for 14 h at room temperature to yield a blue/green mixture. The solvent was removed under vacuum and extracted with toluene (2 x 5 mL), filtered over Celite, concentrated, and placed in a −23 °C freezer to yield a green precipitate (124 mg, 69%). X-ray quality crystals were grown from a concentrated toluene/diethyl ether solution at −23 °C. ^{1}H NMR (C_6D_6, 25 °C): δ −3.36 (s, br, 54H, C(C*H*$_3$)$_3$). ^{31}P{^{1}H} (C_6D_6, 25 °C): δ −495.0.

Method B. A 20 mL scintillation vial was charged with **2S-U-^{t}Bu** (128 mg, 0.119 mmol) and THF (5 mL). A second 20 mL scintillation vial was charged with $ZnCl_2$ (8 mg, 0.0595 mmol) and THF (1 mL) and was added to the **2S-U-^{t}Bu** solution at room temperature and allowed to stir for 14 h to yield a green/yellow solution. The solvent was removed under vacuum, extracted with

toluene, filtered over Celite, concentrated a placed in a −23 °C freezer to yield a green precipitate (59 mg, 55%). NMR spectroscopy data matched spectra reported for *Method A*.

$U(Se_2P^tBu_2)_3Cl$, 4Se-U^{tBu}-Cl. *Method A*. A 20 mL scintillation vial was charged with UCl_4 (96 mg, 0.254 mmol) and CH_3CN (3 mL). A second 20 mL scintillation vial was charged with $KSe_2P^tBu_2$ (269 mg, 0.786 mmol) and was added as solid to UCl_4 at room temperature. The reaction was allowed to stir for 14 h to yield an orange/red precipitate. The solvent was decanted and the solid was dried under vacuum. The orange/red solid was extracted with toluene (2 x 4 mL), filtered over Celite, concentrated, and placed in a −23 ºC freezer to yield a red precipitate (234 mg, 78%). X-ray quality crystals were grown from a concentrated toluene solution at −23 ºC. ^{1}H NMR (C_6D_6, 25 °C): δ −2.31 (s, br, 54H, C(CH_3)$_3$). ^{31}P{^{1}H} (C_6D_6, 25 °C): δ −690.0. IR (cm^{-1}): 2981 (s), 2960 (s) 2941 (s), 2911 (s), 2899 (s), 2866 (m), 1470 (s), 1389 (m), 1363 (s), 1171 (s), 1020 (s), 936 (m), 799 (m), 606 (w), 583 (s), 532 (s), 487 (s). Anal. calcd. for $C_{24}H_{54}ClP_3Se_6U$: C, 24.37%; H, 4.60%. Found C, 24.77%; H, 4.31%.

Method B. A 20 mL scintillation vial was charged with **2Se-U-^{t}Bu** (100 mg, 0.0689 mmol) and THF (3 mL). A second 20 mL scintillation vial was charged with $ZnCl_2$ (4.7 mg, 0.0345 mmol) and added as solid to **2Se-U-^{t}Bu** at room temperature. The reaction was stirred for 14 h to yield a dark red solution. The reaction was filtered over Celite and the solvent was removed under vacuum. The dark red solid was washed with hexanes (2 x 3 mL) and dried. The red solid was extracted with toluene, filtered over Celite, concentrated and placed in a −23 ºC freezer to yield a red precipitate (43 mg, 53%). NMR spectroscopy data matched spectra reported for *Method A*.

$U(Se_2P^tBu_2)_3F$, 5Se-U^{tBu}-F. A 20 mL scintillation vial was charged with **2Se-U-^{t}Bu** (174 mg, 0.120 mmol) and THF (3 mL). A second 20 mL scintillation vial was charged with Hg_2F_2 (26

mg, 0.0592 mmol) and added as solid to **2Se-U-^{t}Bu** at room temperature. The reaction was allowed to stir for 14 h to yield an orange solution. The reaction was filtered over Celite, concentrated, layered with hexane, and placed in a −23 ºC freeze overnight to yield an orange precipitate (85 mg, 61%). ^{1}H NMR (C_6D_6, 25 °C): δ −2.71 (s, br, 54H, C(CH_3)$_3$). ^{31}P{^{1}H} (C_6D_6, 25 °C): δ −786.0. IR (cm^{-1}): 2953 (s), 2907 (s), 2863 (s), 1463 (s), 1393 (w), 1361 (s), 1171 (s), 1099 (m), 1071 (m), 1020 (s), 937 (w), 816 (w), 801 (m), 575 (s), 524 (s), 483 (s). Due to the similar solubility of **5Se-U^{tBu}-F** and the transmetalation byproduct, a suitable element analysis could not be achieved.

U(Se$_2$P^{t}Bu$_2$)$_3$Br, 6Se-U^{tBu}-Br. A 20 mL scintillation vial was charged with **2Se-U-^{t}Bu** (175 mg, 0.121 mmol) and THF (5 mL). A second 20 mL scintillation vial was charged with CuBr (17 mg, 0.121 mmol) and was added as a solid to **2Se-U-^{t}Bu** at room temperature. The reaction was stirred for 14 h, filtered over Celite, concentrated, layered with hexane, and placed in a −23 ºC freeze overnight to yield a dark red precipitate (92 mg, 62%). ^{1}H NMR (C_6D_6, 25 °C): δ −1.39 (s, br, 54H, C(CH_3)$_3$). ^{31}P{^{1}H} (C_6D_6, 25 °C): δ −652.0. IR (cm^{-1}): 2954 (s), 2098 (s), 2864 (s), 1464 (s), 1390 (w), 1362 (m), 1172 (s), 1070 (m), 1021 (s), 936 (w), 841 (w), 802 (m), 581 (m), 530 (m), 484 (s). Due to the similar solubility of **6Se-U^{tBu}-Br** and the transmetalation byproduct, a suitable element analysis could not be achieved.

U(Se$_2$P^{t}Bu$_2$)$_3$I, 7Se-U^{tBu}-I. A 20 mL scintillation vial was charged with **2Se-U-^{t}Bu** (326 mg, 0.225 mmol) and THF (5 mL). A second 20 mL scintillation vial was charged with CuI (86 mg, 0.856 mmol) and added as a solid to **2Se-U-^{t}Bu** at room temperature. The reaction was stirred for 14 h and filtered over Celite, and the solvent was removed under vacuum. The red solid was extracted with hexanes (2 x 3 mL), decanted, and the red precipitate was dried under vacuum. The red solid was extracted with toluene, filtered over Celite, concentrated, and placed in a −23

ºC freeze overnight to yield a dark red precipitate (195 mg, 68%). X-ray quality crystals were grown from a toluene/hexanes mixture at −23 ºC. ^{1}H NMR (C_6D_6, 25 °C): δ −0.30 (s, br, 54H, C(CH_3)$_3$). ^{31}P{^{1}H} (C_6D_6, 25 °C): δ −635.0. IR (cm^{-1}): 2960 (s), 2914 (s), 2899 (s), 2863 (s), 1471 (s), 1389 (m), 1364 (s), 1172 (s), 1079 (m), 1020 (s), 936 (m), 800 (s), 636 (w), 606 (w), 583 (s), 531 (s), 483 (s). Anal. calcd. for $C_{24}H_{54}IP_3Se_6U$: C, 22.62%; H, 4.27%. Found C, 22.60%; H, 4.02%.

[Cu(Se$_2$P^{t}Bu$_2$)]$_4$, 8Se-Cu-^{t}Bu. A 20 mL scintillation vial was charged with [Cu(NCMe)$_4$][PF$_6$] (109 mg, 0.292 mmol) and acetonitrile (3 mL). KSe$_2$P^{t}Bu$_2$ (100 mg, 0.292 mmol) was added to the mixture as a solid at room temperature and the reaction was allowed to stir for 14 h. The solvent was removed under vacuum and the solid was extracted with toluene, filtered over Celite and concentrated. X-ray quality yellow crystals were grown from toluene/hexanes mixture at −23 ºC (two crops, 80 mg, 75%). ^{1}H NMR (C_6D_6, 25 °C): δ 1.51 (d, $^{3}J_{P\text{-}H}$ = 17.0 Hz, 72H, C(CH_3)$_3$). ^{13}C{^{1}H} (C_6D_6, 25 °C): δ 42.18 (d, $^{1}J_{P\text{-}C}$ = 18.0 Hz), 29.32. ^{31}P{^{1}H} (C_6D_6, 25 °C): δ 90.6 (s + d, satellites, $^{1}J_{Se\text{-}P}$ = 533 Hz). IR (cm^{-1}): 2995 (s), 2978 (s), 2961 (s), 2913 (s), 2867 (s), 1465 (s), 1388 (m), 1362 (s), 1173 (s), 1020 (s), 937 (w), 801 (s), 730 (m), 695 (w), 596 (w), 577 (s), 528 (s), 484 (s). Anal. calcd. for $C_{32}H_{72}P_4Se_8Cu_4$•0.5(C_7H_8): C, 28.19%; H, 5.06%. Found C, 28.47%; H, 5.04%.

Table 1. X-ray crystallographic data shown for complexes homoleptic Th(E$_2$PR$_2$)$_4$, E = S, Se; R = ^{i}Pr, ^{t}Bu; and U(S$_2$P^{i}Pr)$_4$

	1S-Th-^{i}Pr	**2S-Th-^{t}Bu**	**1Se-Th-^{i}Pr**	**2Se-Th-^{t}Bu**	**1S-U-^{i}Pr**
CCDC deposit number	1404305	1404306	1404307	1404308	1406602
Empirical formula	$C_{28}H_{64}OP_4S_8Th$	$C_{32}H_{72}P_4S_8Th$	$C_{24}H_{56}P_4Se_8Th$	$C_{32}H_{72}P_4Se_8Th$	$C_{24}H_{56}P_4S_8U$
Formula weight (g/mol)	1029.19	1069.29	1332.28	1444.49	963.16
Crystal habit, color	Brick, colorless	Prism, colorless	Brick, colorless	Prism, colorless	Needle, green
Temperature (K)	100(2)	100(2)	173(2)	100(2)	100(2)
Space group	$P2_1/n$	P-4n2	Cc	P-4n2	$Pnn2$
Crystal system	Monoclinic	Tetragonal	Monoclinic	Tetragonal	Orthorhombic
Volume (Å^3)	4371.1(7)	5194(9)	4143.3(14)	5491.4(9)	8443(3)

a (Å)	16.756(2)	18.090(15)	16.854(3)	18.3858(14)	21.242(4)
b (Å)	13.249(1)	18.090(15)	13.348(3)	18.3858(14)	36.150(6)
c (Å)	20.758(2)	15.871(13)	18.538(4)	16.2449(12)	10.995(2)
α (˚)	90.00	90	90.00	90.00	90.00
β (˚)	108.461(1)	90	96.522(2)	90.00	90.00
γ (˚)	90.00	90	90.00	90.00	90.00
Z	4	4	4	4	4
Calculated density (Mg/m^3)	1.564	1.368	2.136	1.747	1.518
Absorption coefficient (mm^{-1})	3.962	3.336	10.796	8.153	4.407
Final R indices [I > 2σ(I)]	R = 0.0171 R_W = 0.0401	R = 0.0139 R_W = 0.0315	R = 0.0209 R_W = 0.0434	R = 0.0131 R_W = 0.0297	R = 0.0474 R_W = 0.1272

Table 2. X-ray crystallographic data shown for complexes $U(Se_2PR_2)_4$, R = ^{i}Pr, ^{t}Bu; $U(Se_2PR_2)_3Cl$, R = ^{i}Pr, ^{t}Bu; $U(Se_2P^{t}Bu_2)_3I$, and $[Cu(Se_2P^{t}Bu_2)]_4$.

	2Se-U-^{i}Pr	**2Se-U-^{t}Bu**	**3Se-U^{iPr}-Cl**	**4Se-U^{tBu}-Cl**	**7Se-U^{tBu}-I**	**8Se-Cu-^{t}Bu**
CCDC deposit number	1404310	1404312	1404309	1404311	1406600	1404303
Empirical formula	$C_{24}H_{56}P_4Se_8U$	$C_{32}H_{72}P_4Se_8U$	$C_{25}H_{50}ClP_3Se_6U$	$C_{24}H_{54}ClP_3Se_6U$	$C_{24}H_{54}IP_3Se_6U$	$C_{32}H_{72}P_4Se_8Cu_4$
Formula weight (g/mol)	1338.27	1450.48	1190.80	1182.82	1182.82	1466.61
Crystal habit, color	Prism, red	Prism, red	Prism, red	Prism, red	Prism, red	yellow
Temperature (K)	100(2)	100(2)	173(2)	100(2)	100(2)	100(2)
Space group	*C*c	*P*-4n2	*P*212121	*P*212121	*P*212121	*C*2/c
Crystal system	Monoclinic	Tetragonal	Orthorhombic	Orthorhombic	Orthorhombic	Monoclinic
Volume ($Å^3$)	4069.7(4)	5480.4(9)	3825.3(6)	3843.9(9)	3843.9(9)	5984.5(14)
a (Å)	16.7142(10)	18.3367(14)	12.4588(12)	10.7542(15)	10.7542(15)	20.874(3)
b (Å)	13.2787(8)	18.3367(14)	14.4390(14)	16.203(2)	16.203(2)	18.581(3)
c (Å)	18.4521(11)	16.2992(12)	21.264(2)	22.059(3)	22.059(3)	16.759(2)
α (˚)	90	90	90	90	90	90
β (˚)	96.4050(10)	90	90	90	90	112.976(2)
γ (˚)	90	90	90	90	90	90
Z	4	4	4	4	4	4
Calculated density (Mg/m^3)	2.184	1.758	2.068	2.044	2.044	1.628
Absorption coefficient (mm^{-1})	11.316	8.411	10.162	10.112	10.112	6.393
Final R indices [I > 2σ(I)]	R = 0.0159 R_W = 0.0341	R = 0.0145 R_W = 0.0315	R = 0.0187 R_W = 0.0386	R = 0.0175 R_W = 0.0391	R = 0.0277 R_W = 0.0647	R = 0.0203 R_W = 0.0452

Computational Details. All calculations were performed at the density functional theoretical (DFT) level using version 6.6 of the TURBOMOLE quantum chemistry software package.[18] XRD-derived structural parameters were used as the basis for geometry optimizations. The hybrid-GGA PBE0[19] exchange-correlation functional, which incorporates a perturbatively derived 25% contribution of exact exchange, was used throughout. In all calculations, basis sets of polarized triple-ζ quality were used. For geometry optimizations, Ahlrichs-style basis sets[20,21] were employed, incorporating an effective core potential replacing 60 core electrons of the

actinide ion[22]. We have successfully applied this model chemistry in previous studies of f-element complexes.[23,24] All complexes considered in this study were identified as energetic minima through vibrational frequency analysis.

For subsequent analysis of the electron density, all-electron single point energy calculations were performed at the optimized geometries. These calculations replaced the Ahlrichs basis set on the actinide with the SARC basis set of Pantazis and Neese[25] and incorporated scalar relativistic effects via the 2nd order Douglas-Kroll-Hess Hamiltonian. Topological and integrated properties of the resulting electron densities were obtained via application of the Quantum Theory of Atoms in Molecules[26] (QTAIM) as implemented in version 14.11.23 of the AIMAll code.[27]

Results and Discussion

The potassium salts of the dithio- and diselenophosphinate, $KS_2P^tBu_2$, $KSe_2P^iPr_2$, and $KSe_2P^tBu_2$ were synthesized using previously reported procedures, i.e. the deprotonation of the secondary phosphine with potassium hydroxide followed by addition of two equivalents of the elemental chalcogen.[28] All were obtained as white solids in good to excellent yields.

The synthesis of complexes (**1S-Th-^{i}Pr**)-(**1Se-Th-^{t}Bu**) was achieved through the stoichiometric salt metathesis reactions at room temperature (eq 1). Compounds (**2S-Th-^{t}Bu**)-(**2Se-Th-^{t}Bu**) have not been reported previously. The salt metathesis reactions of complexes **1S-Th-^{i}Pr** and **2S-Th-^{t}Bu** yielded colorless solutions while complexes **1Se-Th-^{i}Pr** and **2Se-Th-^{t}Bu** were a yellow hue. The solubility of the diisopropyldichalogenophosphinates and di-*tert*-butyldichalogenophosphinates was greater in toluene and THF, but not soluble in aliphatic hydrocarbons, diethyl ether, or acetonitrile. Synthesis of the $U[S_2P^iPr_2]_4$ (**1S-U-^{i}Pr**) and

$U[S_2P^tBu_2]_4$ (**2S-U-^{t}Bu**) was accomplished through the salt metathesis reactions of $K[S_2PR_2]$, R = ^{i}Pr and ^{t}Bu, respectively, and UCl_4 in THF at −20 ºC (eq 2).

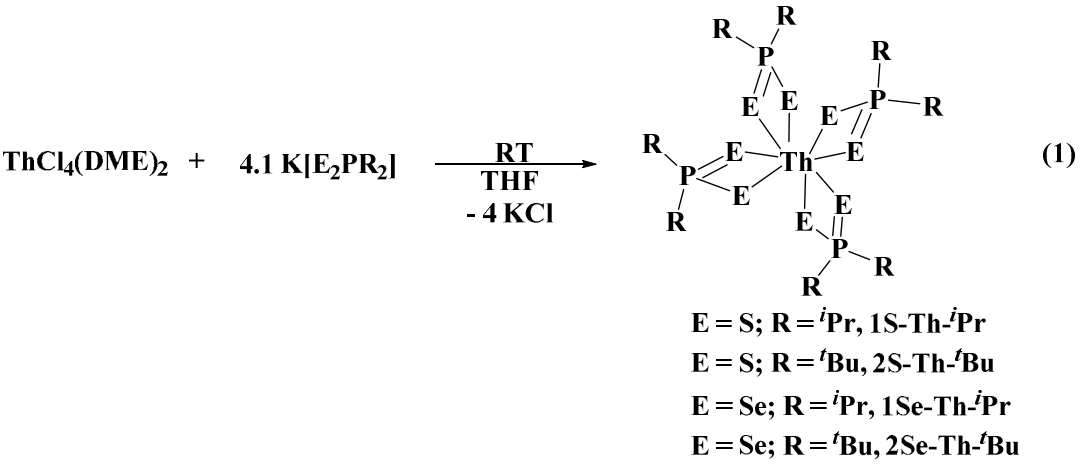

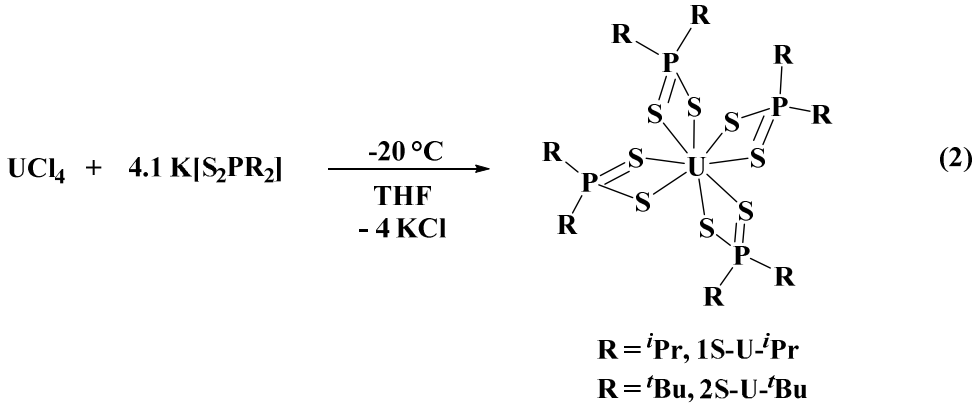

Complex **1S-U-^{i}Pr** was recrystallized from concentrated diethyl ether solution to yield green crystals while complex **2S-U-^{t}Bu** was isolated as a yellow precipitate. The U(IV) homoleptic complex was the exclusive product isolated in reasonable yields: 63% and 54% for **1S-U-^{i}Pr** and **2S-U-^{t}Bu**, respectively. The diisopropyldiselenophosphinate and di-*tert*-butyldiselenophosphinate ligands demonstrated various reactivity dependent on uranium starting material and solvent used. For example, the reaction between UCl_4 and three equivalents of $K[Se_2P^iPr_2]$ in THF at −20 ºC yielded $U[Se_2P^iPr_2]_3Cl$, **3Se-U^{iPr}-Cl**, (eq 3). However, when

$UI_4(1,4\text{-dioxane})_2$ was used, the homoleptic product, $U[Se_2P^iPr_2]_4$, **1Se-U-^{i}Pr**, (eq 4) was isolated. Analogous to these reactions, the ^{t}Bu analogs displayed similar coordination, i.e. $U[Se_2P^tBu_2]_3Cl$, **4Se-U$^{t\mathrm{Bu}}$-Cl** (eq 5), and $U[Se_2P^tBu_2]_4$, **2Se-U-^{t}Bu** (eq 4), were obtained with UCl_4 and $UI_4(1,4\text{-dioxane})_2$, respectively. The homoleptic complexes can be produced from UCl_4 and four equivalents of the respective potassium salts when acetonitrile is used as a solvent. When the reaction between UCl_4 and $K[Se_2P^tBu_2]$ was attempted in THF, a bridging μ_2-oxo complex, μ_2-O$\{U[Se_2P^tBu_2]_3\}_2$, was isolated (see Supporting Information).

$$\mathbf{UCl_4 + 3.1\ K[Se_2P^iPr_2]} \xrightarrow[\text{THF}\ -\ 3\ \text{KCl}]{-20\ ^oC} \quad \textbf{(3)}$$

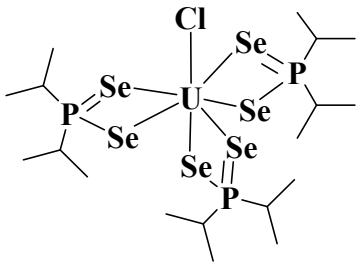

3Se-U$^{i\mathrm{Pr}}$-Cl

$$\mathbf{UI_4(1,4\text{-dioxane})_2 + 4.1\ K[Se_2PR_2]} \xrightarrow[\text{CH}_3\text{CN}\ -\ 4\ \text{KI}]{-20\ ^oC} \quad \textbf{(4)}$$

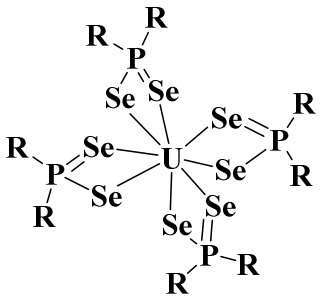

R = ^{i}Pr, 1Se-U-^{i}Pr
R = ^{t}Bu, 2Se-U-^{t}Bu

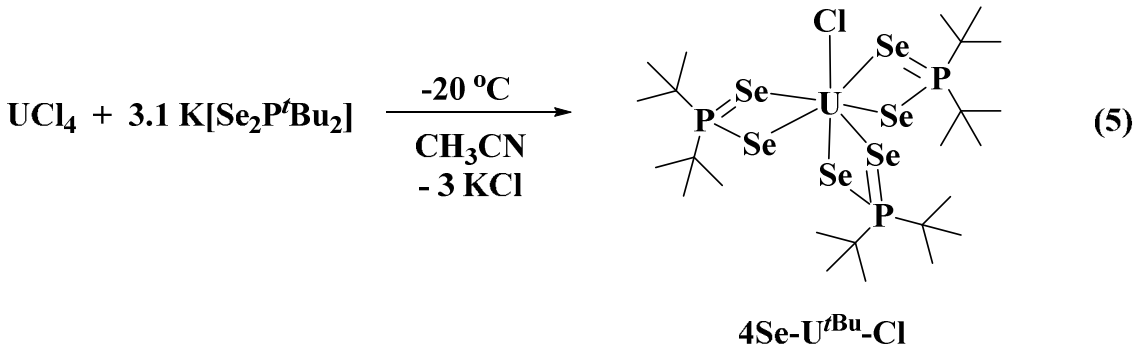

4Se-U$^{t\mathrm{Bu}}$-Cl

The ^{1}H and ^{13}C{^{1}H} spectra for complexes (**1S-Th-^{i}Pr**)-(**2Se-Th-^{t}Bu**) were similar; however, the ^{31}P{H} spectra displayed two significant shifts (Table 3). The ^{31}P{^{1}H} chemical resonances of **1S-Th-^{i}Pr** and **2S-Th-^{t}Bu** occurred at 84.9 and 99.1 ppm, respectively, while ^{31}P{^{1}H} chemical resonances of **1Se-Th-^{i}Pr** and **2Se-Th-^{t}Bu** occurred at 57.6 and 78.3 ppm, respectively. The upfield shift in chemical resonances of **1Se-Th-^{i}Pr** and **2Se-Th-^{t}Bu** can be attributed to the decrease in electronegativity of the selenium atom as compared to the electronegativity of the sulfur atom.[29] The small decrease in the $^{1}J_{\mathrm{Se\text{-}P}}$ of **2Se-Th-^{t}Bu** as compared to **1Se-Th-^{i}Pr** demonstrates the better σ-donating ability of the *tert*-butyl groups to transfer electron density to the phosphorus atom. The ^{77}Se{^{1}H} NMR chemical resonances for **1Se-Th-^{i}Pr** and **2Se-Th-^{t}Bu** were 6.4 and 90.5 ppm, respectively, however, no observable trend could be determined. The only other ^{77}Se{^{1}H} chemical resonance reported for a thorium complex containing a Th-Se bond is Th[Se$_2$P(OMe)Ph]$_4$ (δ = 222 ppm, $^{1}J_{\mathrm{Se\text{-}P}}$ = 580 Hz).[6]

Table 3. ^{31}P{^{1}H} and ^{77}Se{^{1}H} NMR data for complexes (**1S-Th-^{i}Pr**)- (**2Se-Th-^{t}Bu**)

	^{31}P{^{1}H} (δ)	**^{77}Se{^{1}H} (δ)**
Th(S$_2$P^{i}Pr$_2$)$_4$ (**1S-Th-^{i}Pr**)	84.9	---
Th(S$_2$P^{t}Bu$_2$)$_4$ (**2S-Th-^{t}Bu**)	99.1	---
Th(Se$_2$P^{i}Pr$_2$)$_4$ (**1Se-Th-^{i}Pr**)	57.6 (s + d satellites, $^{1}J_{\mathrm{Se\text{-}P}}$ = 500 Hz)	6.4 (d, $^{1}J_{\mathrm{P\text{-}Se}}$ = 500 Hz)
Th(Se$_2$P^{t}Bu$_2$)$_4$ (**2Se-Th-^{t}Bu**)	78.3 (s + d satellites, $^{1}J_{\mathrm{Se\text{-}P}}$ = 491 Hz)	90.5 (d, $^{1}J_{\mathrm{P\text{-}Se}}$ = 491 Hz)

Table 4. ^{1}H and ^{31}P{^{1}H} NMR data for complexes (**1S-U-^{i}Pr**)-(**2Se-U-^{t}Bu**)

	^{1}H (δ)	^{31}P{^{1}H} (δ)
$U(S_2P^iPr_2)_4$ (**1S-U-^{i}Pr**)	8.00 ($CH(CH_3)_2$), 4.20 ($CH(CH_3)_2$)	−436.3
$U(S_2P^tBu_2)_4$ (**2S-U-^{t}Bu**)	−11.90	−467.2
$U(Se_2P^iPr_2)_3Cl$ (**3Se-U^{iPr}-Cl**)	7.33 ($CH(CH_3)_2$), 4.36 ($CH(CH_3)_2$)	−610.2
$U(Se_2P^tBu_2)_3Cl$ (**4Se-U^{tBu}-Cl**)	−2.31	−690.0
$U(Se_2P^iPr_2)_4$ (**1Se-U-^{i}Pr**)	7.34 ($CH(CH_3)_2$), 4.37 ($CH(CH_3)_2$)	−618.0
$U(Se_2P^tBu_2)_4$ (**2Se-U-^{t}Bu**)	2.74	−473.0

The ^{1}H and ^{31}P{^{1}H} NMR spectroscopy of complexes (**1S-U-^{i}Pr**)-(**2Se-U-^{t}Bu**) are listed in Table 4. The ^{1}H spectra for complexes (**1S-U-^{i}Pr**)-(**2Se-U-^{t}Bu**) all exhibited paramagnetically shifted resonances for their respective alkyl groups. The ^{31}P{^{1}H} resonances were also paramagnetically shifted. One noticeable feature in the ^{31}P{^{1}H} is the downfield shift in the chemical resonance of the homoleptic of $U[S_2P^iPr_2]_4$ and $U[S_2P^tBu_2]_4$ as compared to complexes **7-10**. The downfield shift can be explained by the more electronegative sulfur atom bound to the phosphorus as previously mentioned with the homoleptic thorium complexes. The IR spectroscopy experiments were conducted for complexes (**1S-Th-^{i}Pr**)-(**2Se-Th-^{t}Bu**) and selected results are tabulated in Table S3.

The solid-state structures of (**1S-Th-^{i}Pr**)-(**2Se-Th-^{t}Bu**) were determined through X-ray crystallography analysis. Complexes (**1S-Th-^{i}Pr**)-(**2Se-Th-^{t}Bu**) were homoleptic with pseudo C_{4v} symmetry (Figure 1). Each chalcogenide atom is bonded to the thorium metal center given rise to a coordination number of eight for complexes (**1S-Th-^{i}Pr**)-(**2Se-Th-^{t}Bu**) and the geometry can be best described at a triangular dodecahedron for all four complexes.[30] Each $[E_2PR_2]^-$ (E = S, Se; R = ^{i}Pr, ^{t}Bu) ligand is nearly coplanar with the other with a Se1-Se2-Se3-

Se4 dihedral angle of 2.10º and almost orthogonal to the other two with a Se2-Th1-Se4-P2 dihedral angle of 96.90º. No observable Th-P bond was found in complexes (**1S-Th-^{i}Pr**)-(**2Se-Th-^{t}Bu**). A slight deviation in the Th-E bond distances was observed for each $[E_2PR_2]^-$ ligand, one short and one long. This feature was observed for other homoleptic thorium dichalogenide complexes, $Th[S_2P(4\text{-}MeOC_6H_4)(OMe)]_4$ and $Th[Se_2P(C_6H_5)(OMe)]_4$.[6] The Th-E and E-Th-E bond distances and angles are listed in Table 5.

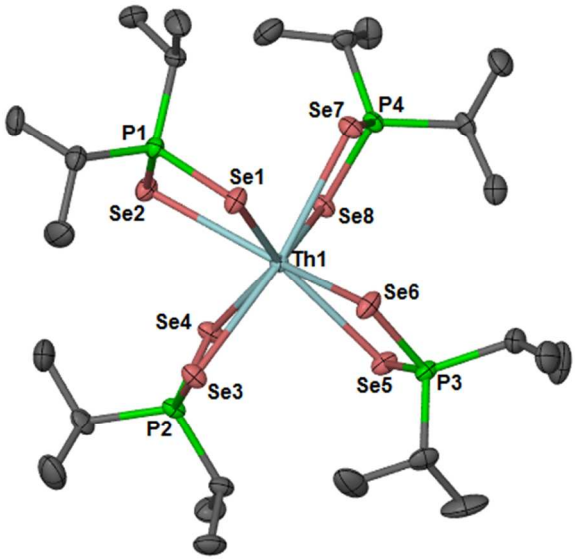

Figure 1. Complex **3** is shown as a representative thermal ellipsoid plot of homoleptic $Th[E_2P^iPr_2]_4$, E = S, Se, complexes. Thermal ellipsoids at 50% and hydrogens omitted for clarity.

Table 5. Selected bond distances (Å) and angles (º) for $Th[S_2P^iPr_2]_4$ (**1S-Th-^{i}Pr**), $Th[S_2P^tBu_2]_4$ (**2S-Th-^{t}Bu**), $Th[Se_2P^iPr_2]_4$ (**1Se-Th-^{i}Pr**), and $Th[Se_2P^tBu_2]_4$ (**2Se-Th-^{t}Bu**).

	1S-Th-^{i}Pr	**2S-Th-^{t}Bu**		**1Se-Th-^{i}Pr**	**2Se-Th-^{t}Bu**
Th1-S1	2.8780(6)	2.929(3)	Th1-Se1	3.0576(7)	3.0636(6)
Th1-S2	2.9190(6)	2.944(2)	Th1-Se2	3.0107(6)	3.0612(7)
Th1-S3	2.9307(6)	2.915(2)	Th1-Se3	3.0023(6)	3.0291(6)
Th1-S4	2.9338(6)	2.940(2)	Th1-Se4	3.0477(7)	3.0653(7)
Th1-S5	2.9198(5)	-	Th1-Se5	3.0379(6)	-
Th1-S6	2.8882(5)	-	Th1-Se6	3.0492(7)	-

Th1-S7	2.8728(5)	-	Th1-Se7	3.0308(6)	-
Th1-S8	2.9182(5)	-	Th1-Se8	3.0659(6)	-
S1-Th1-S2	69.465(14)	67.07(4)	Se1-Th1-Se2	71.561(15)	69.189(16)
S3-Th1-S4	68.393(14)	67.30(5)	Se3-Th1-Se4	71.829(16)	69.544(16)
S5-Th1-S6	68.985(15)	-	Se5-Th1-Se6	70.737(17)	-
S7-Th1-S8	69.195(15)	-	Se7-Th1-Se8	70.454(16)	-
S1-P1-S2	109.76(3)	106.79(10)	Se1-P1-Se2	109.08(5)	105.63(7)
S3-P2-S4	109.59(3)	106.74(10)	Se3-P2-Se4	109.87(5)	105.55(7)
S5-P3-S6	109.30(3)	-	Se5-P3-Se6	108.64(5)	-
S7-P4-S8	109.33(3)	-	Se7-P4-Se8	108.32(5)	-

The average Th-S bond distance was 2.9075(5) Å and 2.932(2) Å for complexes **1S-Th-^{i}Pr** and **2S-Th-^{t}Bu**, respectively, while the average Th-Se bond distance was 3.0377(6) Å and 3.0548(8) Å for complexes **1Se-Th-^{i}Pr** and **2Se-Th-^{t}Bu**, respectively. Complexes **1Se-Th-^{i}Pr** and **2Se-Th-^{t}Bu** represent only the second and third structurally characterized homoleptic complexes containing a Th-Se linkage and compares well to the first homoleptic thorium complex with selenium atoms, $Th[Se_2P(C_6H_5)(OMe)]_4$, the average Th-Se distance of 3.0261(4) Å.[6] These bond distances are longer than those in $(1,2,4\text{-}^{t}Bu_3C_5H_2)_2Th(SePh)_2$ and $(1,2,4\text{-}^{t}Bu_3C_5H_2)Th(SePh)_3(bipy)$ reported average Th-Se distances of 2.938(8)[31] and 2.877 Å,[32] respectively. The elongated Th-Se bonds in the homoleptic compounds arise from the negative charge spread over two donor atoms.

The homoleptic U(IV) complexes (**1S-U-^{i}Pr**, **1Se-U-^{i}Pr** and **2Se-U-^{t}Bu**) are isostructural with the thorium analogs (Figure 2) with selected bond distances and angles listed in Table 6. The IR spectroscopy experiments were conducted for complexes **1S-U-^{i}Pr**, **2S-U-^{t}Bu**, **1Se-U-^{i}Pr**, and **2Se-U-^{t}Bu** and selected results are tabulated in Table S4.

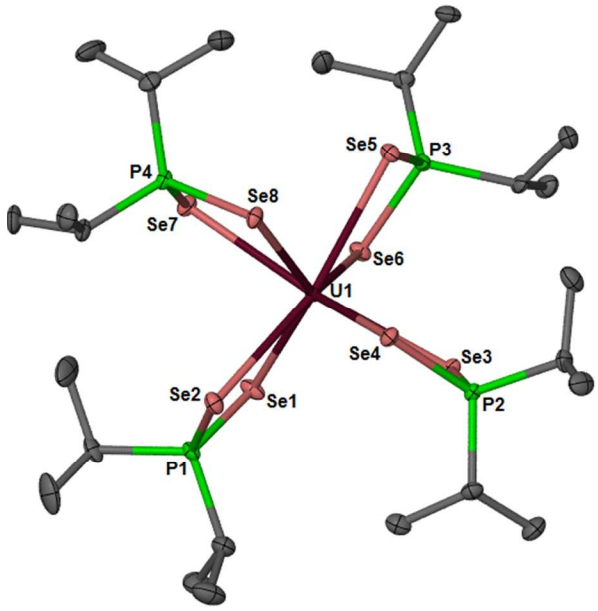

Figure 2. Complex **1Se-U-^{i}Pr** is shown as a representative thermal ellipsoid plot of homoleptic $U[E_2P^iPr_2]_4$, E = S, Se, complexes. Thermal ellipsoids at 50% and hydrogens omitted for clarity.

Table 6. Selected bond distances (Å) and angles (°) for $U[S_2P^iPr_2]_4$ (**1S-U-^{i}Pr**), $U[Se_2P^iPr_2]_4$ (**1Se-U-^{i}Pr**), and $U[Se_2P^tBu_2]_4$ (**2Se-U-^{t}Bu**).

	1S-U-^{i}Pr		**1Se-U-^{i}Pr**	**2Se-U-^{t}Bu**
U1-S1	2.885(3)	U1-Se1	3.0076(4)	2.9973(10)
U1-S2	2.809(3)	U1-Se2	2.9859(4)	3.0204(11)
U1-S3	2.809(3)	U1-Se3	3.0263(4)	3.0318(11)
U1-S4	2.879(4)	U1-Se4	3.0477(7)	2.9601(10)
U1-S5	2.876(3)	U1-Se5	2.9362(4)	-
U1-S6	2.840(3)	U1-Se6	3.0192(4)	-
U1-S7	2.843(4)	U1-Se7	2.9343(4)	-
U1-S8	2.842(4)	U1-Se8	3.0092(4)	-
S1-U1-S2	70.49(9)	Se1-U1-Se2	71.561(15)	69.90(3)
S3-U1-S4	70.37(10)	Se3-U1-Se4	71.017(10)	70.10(3)
S5-U1-S6	70.03(10)	Se5-U1-Se6	72.575(10)	-
S7-U1-S8	70.28(11)	Se7-U1-Se8	71.302(11)	-
S1-P1-S2	109.01(19)	Se1-P1-Se2	106.99(4)	104.44(11)
S3-P2-S4	109.1(2)	Se3-P2-Se4	106.99(4)	104.06(11)
S5-P3-S6	109.1(2)	Se5-P3-Se6	108.24(4)	-
S7-P4-S8	104.6(3)	Se7-P4-Se8	108.70(4)	-

Complexes **3Se-U^{iPr}-Cl** and **4Se-U^{tBu}-Cl** both contain one chloride ligand, however, the remaining $[Se_2PR_2]^-$ (R = ^{i}Pr, ^{t}Bu) ligands adopt very different geometries around the uranium metal center (Figures 3 and 4). For complex **3Se-U^{iPr}-Cl**, two of the $[Se_2P^iPr_2]^-$ ligands are nearly coplanar with each other with Se3-Se4-Se6-Se5 dihedral angle of 2.42º. The third $[Se_2P^iPr_2]^-$ ligand is almost orthogonal to the other two with a Se6-U1-Se2-P1 dihedral angle of 87.02º. This geometric arrangement is the likely result of minimizing the unfavorable interactions between the isopropyl groups on the phosphorus atoms. Another unique feature exclusive to **3Se-U^{iPr}-Cl** is the U1-Se1 and U1-Se2 bond distances (Table 7). The U1-Se1 bond length is 2.9003(5) Å while the U1-Se2 3.0038(5) Å. As in the thorium complexes, these are elongated with respect to other mononuclear U(IV) complexes such as 2.7897(7) and 2.8597(8) Å in [K(18-crown-6)][$(R_2N)_3U(\eta^2$-$Se_2)$], R = $SiMe_3$,[33] or 2.8432(7) Å in $(C_5Me_5)_2U(SePh)_2$.[34] In complex **4Se-U^{tBu}-Cl**, the Se3-Se4-Se6-Se5 dihedral angle of 68.39º and a U1-Se1 and U1-Se2 bond distances of 2.9548(10) and 2.9507(11) Å, respectively. The U1-Cl1 distances in **3Se-U^{iPr}-Cl** and **4Se-U^{tBu}-Cl** are 2.5632(12) and 2.587(2) Å, respectively and shorter than 2.637 Å in $(C_5Me_4H)_3UCl$,[35] 2.6099(15) Å in $(C_5Me_5)_2U(Cl)(NPh_2)$,[36] and 2.6783(10) Å in $\{U[MeC(NCy)_2]_3Cl\}$.[37]

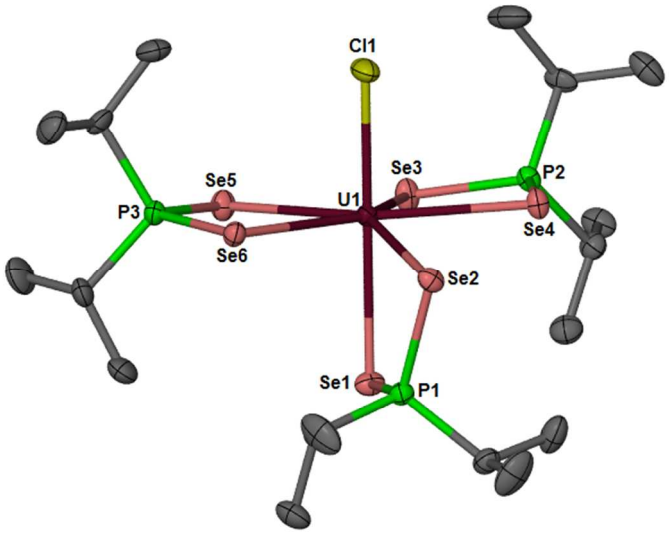

Figure 3. Thermal ellipsoid plot of $U(Se_2P^iPr_2)_3Cl$ (**3Se-U^{iPr}-Cl**). Thermal ellipsoids at 50% and hydrogens omitted for clarity.

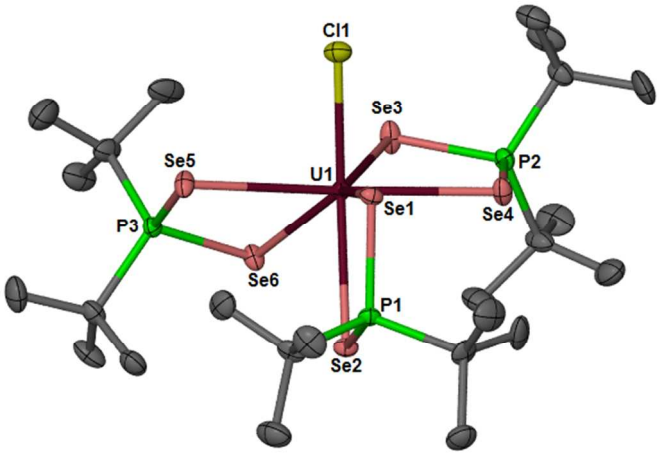

Figure 4. Thermal ellipsoid plot of $U(Se_2P^tBu_2)_3Cl$ (**4Se-U^{tBu}-Cl**). Thermal ellipsoids at 50% and hydrogens omitted for clarity.

Table 7. Selected bond distances (Å) and angles (º) for $U(Se_2P^iPr_2)_3Cl$ (**3Se-U^{iPr}-Cl**) and $U(Se_2P^tBu_2)_3Cl$ (**4Se-U^{tBu}-Cl**).

	3Se-U^{iPr}-Cl	**4Se-U^{tBu}-Cl**
U1-Cl1	2.5632(12)	2.587(2)
U1-Se1	2.9003(5)	2.9548(10)
U1-Se2	3.0038(5)	2.9507(11)
U1-Se3	2.9228(5)	2.9773(10)
U1-Se4	2.9146(5)	2.9136(11)
U1-Se5	2.9599(5)	2.9329(11)
U1-Se6	2.9410(5)	2.9483(10)
Cl1-U1-Se1	173.09(3)	77.41(6)
Cl1-U1-Se2	98.18(3)	149.67(6)
Se1-U1-Se2	75.374(13)	69.90(3)
Se3-U1-Se4	74.228(14)	72.51(3)
Se5-U1-Se6	73.479(14)	73.35(3)
Se1-P1-Se2	111.54(5)	106.34(11)
Se3-P2-Se4	108.18(5)	106.55(11)
Se5-P3-Se6	108.58(5)	107.53(11)

The reactivity of **2Se-Th-^{t}Bu** was investigated through transmetalation reactions with various copper salts ($CuCl_2$, CuBr, and CuI). Interestingly, based on the ^{1}H NMR spectrum, only starting material was observed after letting the reaction stir for 24 h at room temperature. In an attempt to

explain the dearth of reactivity exhibited by **2Se-Th-^{t}Bu**, we compared the averaged difference in the An-Se bond (Δ, [Th-Se] – [U-Se]) in **2Se-Th-^{t}Bu** and **2Se-U-^{t}Bu** to the decrease in ionic radii from an eight coordinate Th^{4+} (1.190 Å) to U^{4+} (1.140 Å).[38] The difference in ionic radii for an eight coordinate Th^{4+} to U^{4+} is *c.a.* 0.050 Å and the Δ value we obtained was 0.052 Å showing there is no difference in the An-Se bond distance between Th and U. A closer comparison of the Th-Se and U-Se bond ranges between **2Se-Th-^{t}Bu** and **2Se-U-^{t}Bu** resulted in a greater range for $U[Se_2P^tBu_2]_4$. The U-Se bond lengths span from 2.9973(10) to 3.0318(11) Å and the Th-Se bond lengths from 3.0291(6) to 3.0653(7) Å. We also compared the average U-Se bond length of $[U(Se_2PPh_2)_4]$[5] to the average U-Se bond lengths in **1Se-U-^{i}Pr** and **2Se-U-^{t}Bu**. We found that replacement of the phenyl ligand for *iso*-propyl and *tert*-butyl ligands resulted in an increase of the U-Se bond length by 0.0279 Å and 0.0345 Å, respectively. The increase in U-Se bond distances for **1Se-U-^{i}Pr** and **2Se-U-^{t}Bu** can be attributed to the steric repulsions provided by the *iso*-propyl and *tert*-butyl ligands making **2Se-U-^{t}Bu** better suited to undergo transmetalation reactions.

Presumably due to steric considerations of the dithio- and diselenophosphinate complexes of uranium, complex **2Se-U-^{t}Bu** displayed a wide array of reactivity with various Cu(I) salts (eq 6). The transmetalation reactions with Cu(I) halides resulted in dark red color change with concomitant formation of $[Cu(Se_2P^tBu_2)]_4$, **8Se-Cu-^{t}Bu**. Complex **8Se-Cu-^{t}Bu** was independently synthesized from the stoichiometric reaction between $[Cu(NCMe)_4][PF_6]$ and $K(Se_2P^tBu_2)$ in acetonitrile. The ^{1}H NMR spectrum showed one doublet centered at 1.51 ppm with $^3J_{P\text{-}H}$ = 17.0 Hz representing the *tert*-butyl protons. The $^{31}P\{^1H\}$ spectrum displayed a singlet at 90.6 ppm with ^{77}Se satellites and $^1J_{Se\text{-}P}$ = 533 Hz. The solid-state structure of **8Se-Cu-^{t}Bu** was solved using X-ray quality crystals grown from a concentrated toluene/hexanes mixture

at −20 ºC (Figure 5). Complex **8Se-Cu-^{t}Bu** is a tetranuclear cluster with Cu1-Se1 bond distance of 2.3862(14) Å and Cu2-Se4 bond distance of 2.3986(14) Å (Table 8). Each $[Se_2P^tBu_2]^-$ ligand is bridging rather than chelating. In one $[Se_2P^tBu_2]^-$ motif, each selenium atom is bound to a phosphorus atom and two different copper atoms, while one selenium atom is bound to one copper metal and a phosphorus atom in the second $[Se_2P^tBu_2]^-$ ligand. Therefore, each copper center is coordinated by three selenium atoms resulting in a cubane structure. The Se-Cu-Se angles span from 126.54(5) to 104.55(5)º placing the copper atoms a distorted trigonal planar geometry. A similar structure, $[Cu(Se_2P^iPr_2)]_4$, has been previous characterized.[39]

To rule out the possibility of a redox reaction occurring between uranium and copper, a non-redox active metal, Zn^{2+}, was attempted (eq 7). The reaction between **2Se-U-^{t}Bu** and half equivalent of $ZnCl_2$ resulted in a red solution and the ^{1}H and ^{31}P{^{1}H} NMR spectra showed the formation of **4Se-U^{tBu}-Cl** as well as a second product (Figure S9). The product was identified as $Zn(Se_2P^tBu_2)_2$ and was independently synthesized from the reaction between $ZnCl_2$ and two equivalents of $KSe_2P^tBu_2$ (See Supporting Information). ^{1}H and ^{31}P{^{1}H} NMR spectroscopy as well as X-ray crystallography confirmed the identity of the $Zn(Se_2P^tBu_2)_2$ product. An additional transmetalation reaction was attempted using Hg_2F_2 to yield the mono-fluoride complex, **5Se-U^{tBu}-F** (eq 7). To disseminate the mercury byproduct, the independent stoichiometric reaction between Hg_2F_2 and $KSe_2P^tBu_2$ was conducted and ^{1}H and ^{31}P{^{1}H} NMR spectroscopy matched the resonance in the transmetalation reaction (See Supporting Information). We are still unclear as to the reason for reactivity of **2Se-U-^{t}Bu** with Cu(I), $ZnCl_2$, and Hg_2F_2 salts. It would seem that an redox event involving a U(V) intermediate can be ruled out on the basis of a successful transmetalation reaction with non-redox active $ZnCl_2$ salt. Given that **2Se-Th-^{t}Bu** and **2Se-U-^{t}Bu** have nearly identical actinide-selenium bond distances, we make the argument that because of

the smaller ionic radius of U(IV), **2Se-U-^{t}Bu** is undergoing something similar to a sterically induced transmetalation reaction with Cu(I), $ZnCl_2$, and Hg_2F_2 salts to yield the heteroleptic mono-halide complexes to relieve steric strain. This type of sterically induced reactivity is known to f elements,[40-44] and has been argued before in the coordination chemistry of Cyanex 301 with actinides.[45]

This is not the first time group 11 salts have been used in actinide chemistry. For example, previous reports have used copper and gold salts to oxidize U(III) to U(IV)[46-49] or U(IV) to U(V).[50-53] Alternatively, the Evans group made use of copper (CuX) and silver (AgX) salts for transmetalation reactions with $(C_5Me_5)_2U(CH_3)_2$ to yield complexes of the form $(C_5Me_5)_2U(CH_3)X$, X = Br, I, OTf.[54,55] We are unaware of any reports of actinides with mercury salts and this provides a new avenue into synthesizing non-organometallic uranium(IV)-fluoride bonds[56-60] which are important in the nuclear fuel cycle.

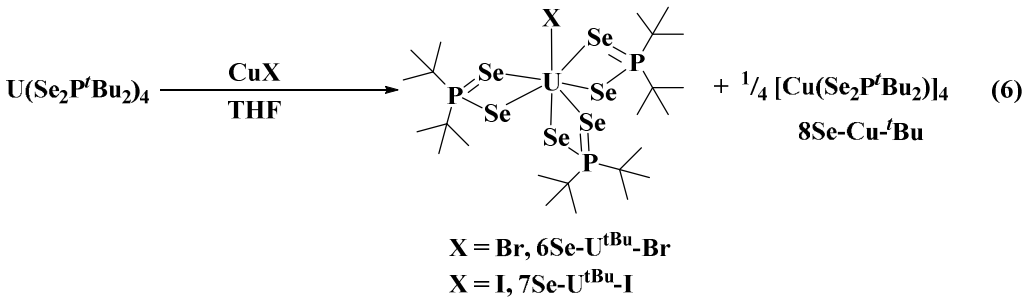

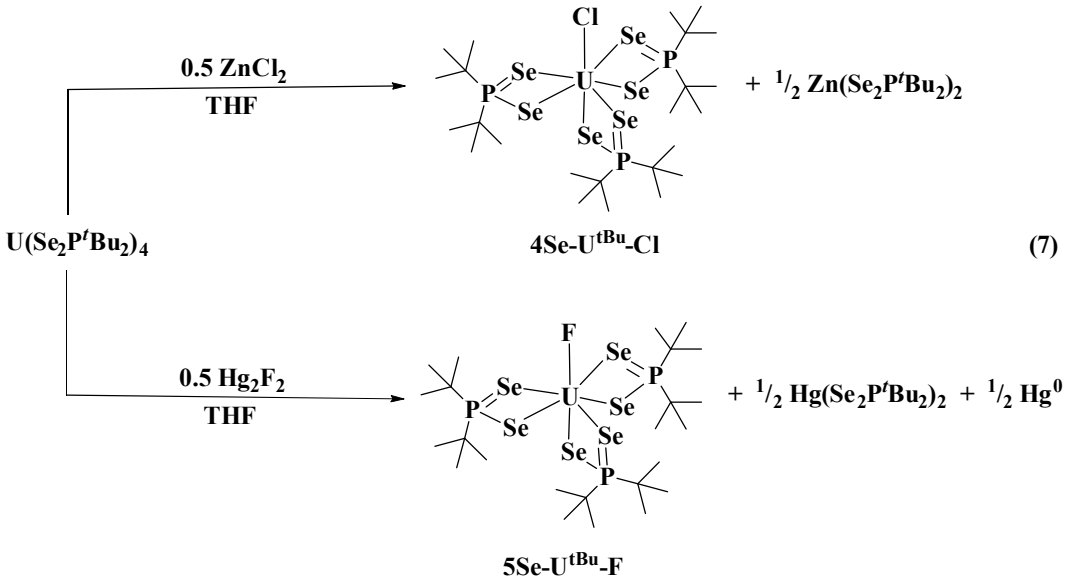

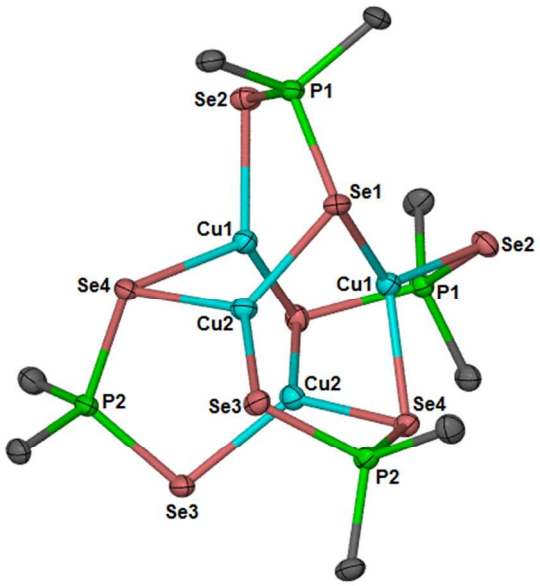

Figure 5. Thermal ellipsoid plot of $[Cu(Se_2P^tBu_2)]_4$ (**8Se-Cu-^{t}Bu**). Thermal ellipsoids at 50% with *tert*-butyl carbons and hydrogens omitted for clarity.

Table 8. Selected bond distances (Å) and angles (º) for $[Cu(Se_2P^tBu_2)]_4$ (**8Se-Cu-^{t}Bu**).

Cu1-Se1	2.3862(14)
Cu1-Se2	2.4233(13)
Cu1-Se4	2.4325(13)
Cu2-Se1	2.4233(13)
Cu2-Se3	2.4216(14)
Cu2-Se4	2.3986(14)

P1-Se1	2.227(2)
P1-Se2	2.9198(13)
P2-Se3	2.161(2)
P2-Se4	2.232(2)
Se1-Cu1-Se2	126.54(5)
Se1-Cu1-Se4	117.82(5)
Se2-Cu1-Se4	107.85(5)
Se1-Cu2-Se3	104.55(5)
Se1-Cu2-Se4	123.48(5)
Se3-Cu2-Se4	125.21(5)
Se1-P1-Se2	113.35(10)
Se3-P2-Se4	113.89(10)

Complexes **5Se-U^{tBu}-F**, **4Se-U^{tBu}-Cl**, **6Se-U^{tBu}-Br**, and **7Se-U^{tBu}-I** were characterized spectroscopically. Table 9 lists the ^{1}H and ^{31}P{^{1}H} chemical shifts and the relationship between the chemical shift of the *tert*-butyl protons and the ancillary X-type ligand (X = F, Cl, Br, I) can be observed. The chemical shift of the *tert*-butyl protons is more upfield with substitution of a stronger π-donor halide ligand (F > Cl > Br >I). This effect can be explained through the stronger shielding experienced by the *tert*-butyl protons as a result of more electron density at the uranium center (i.e. the stronger π-donor, the more electron density at the uranium center). A similar feature is observed the ^{31}P{^{1}H} resonances for the same reason. Similar trends have been noted for various U(III)[61] and U(IV)[36,62,63] complexes.

Table 9. ^{1}H ^{31}P{^{1}H} and NMR data for complexes **5Se-U^{tBu}-F**, **4Se-U^{tBu}-Cl**, **6Se-U^{tBu}-Br**, and **7Se-U^{tBu}-I**

	^{1}H (δ), ^{t}Bu*H*	^{31}P{^{1}H} (δ)
U(Se$_2$P^{t}Bu$_2$)$_3$F (**5Se-U^{tBu}-F**)	−2.71	−786.0
U(Se$_2$P^{t}Bu$_2$)$_3$Cl (**4Se-U^{tBu}-Cl**)	−2.31	−690.0
U(Se$_2$P^{t}Bu$_2$)$_3$Br (**6Se-U^{tBu}-Br**)	−1.39	−652.0
U(Se$_2$P^{t}Bu$_2$)$_3$I (**7Se-U^{tBu}-I**)	−0.30	−635.0.

The solid-state structure of **7Se-U^{tBu}-I** is shown in Figure 6. The U1-I1 bond distance is 3.1187(9) Å and is comparable to other U(IV)-I bond lengths of 3.0603(13) and 3.034(2) Å for

UI(DME) $(NC[^{t}Bu]Mes)_3$ and $(C_5{}^{t}Bu_4H)_3UI$, respectively.[64,65] Table 10 lists the selected bond lengths (Å) and angles (º) for **7Se-U^{tBu}-I**. Complex **7Se-U^{tBu}-I** has a Se3-Se4-Se6-Se5 dihedral angle of 119.4º and is larger than **4Se-U^{tBu}-Cl**. The U-Se bond lengths range from 2.9312(13)-2.8940(13) Å for **7Se-U^{tBu}-I** and are marginally shorter than **4Se-U^{tBu}-Cl**. The increase in dihedral angle of **7Se-U^{tBu}-I** and shorter U-Se bonds can be related to weaker π-donor abilities of the iodide ligand compared to those of the chloride ligand.

Table 10. Selected bond distances (Å) and angles (º) for $U(Se_2P{}^{t}Bu_2)_3I$ (**7Se-U^{tBu}-I**).

U1-I1	3.1187(9)
U1-Se1	2.9038(14)
U1-Se2	2.9312(13)
U1-Se3	2.9263(13)
U1-Se4	2.9293(13)
U1-Se5	2.9198(13)
U1-Se6	2.8940(13)
I1-U1-Se1	72.15(3)
I1-U1-Se2	138.53(3))
Se1-U1-Se2	73.83(4)
Se3-U1-Se4	73.48(4)
Se5-U1-Se6	74.19(4)
Se1-P1-Se2	106.50(15)
Se3-P2-Se4	106.57(13)
Se5-P3-Se6	106.93(14)

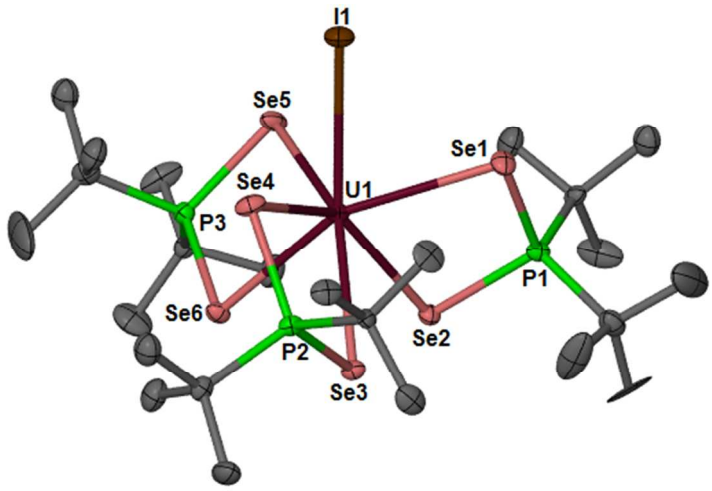

Figure 6. Thermal ellipsoid plot of $U(Se_2P^tBu_2)_3I$ (**7Se-U^{tBu}-I**). Thermal ellipsoids at 50% and hydrogens omitted for clarity.

Electronic Structure Calculations. M-E bond lengths, averaged over the eight bonds in each complex, are compared in Table S5. Theoretical values are in very good agreement with experiment, with the largest difference being 0.016 Å in **1Se-Th-^{i}Pr** and many values differing by less than 0.01 Å. When taking the mean average deviation in bond length for a given complex into account, experimental and theoretical values overlap, justifying the choice of model chemistry.

To examine the electronic structure of these complexes, the Quantum Theory of Atoms in Molecules (QTAIM) approach was performed, in analogy with previous studies. Properties of the electron density at QTAIM derived An-E bond critical points (BCPs) are summarized in Table 11. While these properties are indicative of predominantly ionic interactions, BCP densities are higher in uranium complexes than in thorium analogues, implying greater covalency in the former. Coordination by sulfur also results in BCP densities higher than those found for metal-selenium bonds. These trends, which are mirrored by the BCP energy densities *H*, are as seen previously,[6] although the difference between values obtained for uranium and

thorium complexes is less pronounced here. Interestingly, all ^{i}Pr derivatives exhibit higher degrees of covalency than ^{t}Bu derivatives. This is commensurate with the variation in bond lengths, but is presumably due to steric rather than electronic effects.

Table 11. Topological properties at the M-E bond critical points (BCPs) of the PBE0-derived electron densities. ρ = electron density, $\nabla^2\rho$ = Laplacian of the density, H = energy density. All values are in a.u.

Complex	ρ		$\nabla^2\rho$		H	
	E = S	E = Se	E = S	E = Se	E = S	E = Se
$Th(E_2P^tBu_2)_4$	0.044	0.040	0.065	0.050	-7.4×10^{-3}	-6.5×10^{-3}
$U(E_2P^tBu_2)_4$	0.047	0.042	0.076	0.059	-7.9×10^{-3}	-6.9×10^{-3}
$Th(E_2P^iPr_2)_4$	0.046	0.041	0.068	0.051	-8.0×10^{-3}	-6.8×10^{-3}
$U(E_2P^iPr_2)_4$	0.050	0.043	0.080	0.060	-8.9×10^{-3}	-7.2×10^{-3}

The QTAIM definition of an atom allows for the evaluation of both one- and two-electron integrated properties. The atomic charge q (a one-electron property) and the localization and delocalization indices λ and δ (two-electron properties) are summarized for U, Th, S and Se in Table 12. These data again support the characterization of uranium as exhibiting greater covalent character than thorium. In all complexes, delocalization indices (the number of electrons shared between two atoms), which can be considered an alternative measure of covalent character,[6,66,67] are ~0.05 a.u. greater in uranium complexes than in the thorium analogues. It has previously been noted that the difference between atomic number Z and localization index λ correlates with oxidation state in f-element complexes[66,67] and we also find this correlation here: Z - λ values fall in the range 4.15 - 4.29, close to the formal +4 oxidation state.

Table 12. Integrated QTAIM properties of the PBE0-derived electron densities. q = atomic charge, λ = localization index, δ = delocalization index. All values are in a.u.

Complex	E = S				E = Se			
	q(An)	λ(M)	q(E)	δ(An, E)	q(An)	λ(An)	q(E)	δ(An, E)
$Th(E_2P^tBu_2)_4$	+2.45	85.77	-0.883	0.414	+2.29	85.85	-0.563	0.431

$U(E_2P^tBu_2)_4$	+2.27	87.74	-0.857	0.461	+2.09	87.82	-0.533	0.481
$Th(E_2P^iPr_2)_4$	+2.45	85.75	-0.923	0.420	+2.29	85.84	-0.577	0.432
$U(E_2P^iPr_2)_4$	+2.27	87.71	-0.905	0.471	+2.10	87.81	-0.549	0.484

In contrast to ρ_{BCP} values, delocalization indices suggest the An-Se bonds to be more covalent than the An-S bonds. This was previously observed in other dithiophosphinate and diselenophosphinate actinide complexes,[6] and was rationalized by arguing that ρ_{BCP} is strongly sensitive to bond length, in which there is significant variation between the An-S and An-Se bonds. Bearing in mind the delocalization indices and previous analysis,[6] we therefore conclude the An-Se bonds in these complexes to exhibit marginally more covalent character than the An-S analogues.

Overall, we have synthesized a series of dithio- and diselenophosphinate complexes of thorium(IV) and uranium(IV). The alkyl-substituents on the phosphinate ligands provide insight into the structure and bonding of Cyanex 301 as an extractor ligand. Further spectroscopic analysis is needed to verify the nature of the calculations presented; however, the nature of actinide-ligand bonding remains a fascinating and emerging field.

Conclusions

In summary, we have synthesized and characterized a series of homoleptic $An[E_2PR_2]_4$ (An = Th, U; E = S, Se; R = ^{i}Pr, ^{t}Bu) complexes spectroscopically and determined their structures using X-ray crystallography. Using the QTAIM approach, the electronic structure of these complexes showed increasing covalent bonding character in actinide-selenium bonds than in the corresponding actinide-sulfur bonds. Interestingly, the isopropyl complexes showed a higher degree of covalency than the *tert*-butyl substituents. For the first time, reactivity was demonstrated with these type of complexes using transmetalation reactions between $U(Se_2P^tBu_2)_4$ and Cu^{1+}, $ZnCl_2$, Hg_2F_2 or $HgCl_2$ salts, resulting in the formation of $U[Se_2P^tBu_2]_3$-

X (X = F, Cl, Br, I). The coordination chemistry of soft donor ligands with thorium and uranium is becoming an increasingly studied area and the results presented here add to the intrigue that such oxophilic metal centers can show more covalent bonding character with increasing softer donor atoms.

Supporting Information

Crystallographic details, synthesis and characterization of $Zn(Se_2P^tBu_2)_2$, $Hg(Se_2P^tBu_2)_2$, and thermal ellipsoid plots as well as tables of IR spectroscopy are available free of charge via the Internet at http://pubs.acs.org.

Corresponding Authors

Email: walenskyj@missouri.edu; a.kerridge@lancaster.ac.uk

Acknowledgements

This material is based upon work supported by the U.S. Department of Homeland Security under Grant Award Number, 2012-DN-130-NF0001-02. The views and conclusions contained in this document are those of the authors and should not be interpreted as necessarily representing the official policies, either expressed or implied, of the U.S. Department of Homeland Security. AK thanks the EPSRC for the award of a Career Acceleration Fellowship (Grant Award Number EP/J002208/1) and the NSCCS for access to the 'slater' HPC facility. We also thank Dr. Charles L. Barnes for his assistance with X-ray crystallography.

References

(1) Hudson, M. J.; Harwood, L. M.; Laventine, D. M.; Lewis, F. W. *Inorg. Chem.* **2013**, *52*, 3414.
(2) Kolarik, Z. *Chem. Rev.* **2008**, *108*, 4208.

(3) Lewis, F. W.; Hudson, M. J.; Harwood, L. M. *Synlett* **2011**, *2011*, 2609.
(4) Peterman, D. R.; Law, J. D.; Todd, T. A.; Tillotson, R. D., *Separations for the Nuclear Fuel Cycle in the 21st Century,* **2009**, *ACS Symposium Series*, 251

(5) Jones, M. B.; Gaunt, A. J.; Gordon, J. C.; Kaltsoyannis, N.; Neu, M. P.; Scott, B. L. *Chem. Sci.* **2013**, *4*, 1189.
(6) Behrle, A. C.; Barnes, C. L.; Kaltsoyannis, N.; Walensky, J. R. *Inorg. Chem.* **2013**, *52*, 10623.
(7) Lescop, C.; Arliguie, T.; Lance, M.; Nierlich, M.; Ephritikhine, M. *J. Organomet. Chem.* **1999**, *580*, 137.
(8) Matson, E. M.; Breshears, A. T.; Kiernicki, J. J.; Newell, B. S.; Fanwick, P. E.; Shores, M. P.; Walensky, J. R.; Bart, S. C. *Inorg. Chem.* **2014**, *53*, 12977.
(9) Lam, O. P.; Franke, S. M.; Heinemann, F. W.; Meyer, K. *J. Am. Chem. Soc.* **2012**, *134*, 16877.
(10) Lane, A. C.; Vollmer, M. V.; Laber, C. H.; Melgarejo, D. Y.; Chiarella, G. M.; Fackler, J. P.; Yang, X.; Baker, G. A.; Walensky, J. R. *Inorg. Chem.* **2014**, *53*, 11357.
(11) Cantat, T.; Scott, B. L.; Kiplinger, J. L. *Chem. Commun.* **2010**, *46*, 919.
(12) Gray, D. L.; Backus, L. A.; Krug von Nidda, H.-A.; Skanthakumar, S.; Loidl, A.; Soderholm, L.; Ibers, J. A. *Inorg. Chem.* **2007**, *46*, 6992.
(13) Pinkerton, A. A.; Storey, A. E.; Zellweger, J. *J. Chem. Soc., Dalton Trans.* **1981**, 1475.
(14) Artemev, A. V.; Malysheva, S. F.; Gusarova, N. K.; Trofimov, B. A. *Synthesis* **2010**, 2463.
(15) APEX2 Suite, Bruker AXS Inc, **2006**, Madison, WI
(16) Sheldrick, G. *Acta Cryst.* **2015**, *71*, 3.
(17) Barbour, L. J. *Supramol. Chem.* **2001**, *1*, 189.
(18) Ahlrichs, R.; Bär, M.; Häser, M.; Horn, H.; Kölmel, C. *Chem. Phys. Lett.* **1989**, *162*, 165.
(19) Adamo, C.; Barone, V. *J. Chem. Phys.* **1999**, *110*, 6158.
(20) Weigend, F.; Ahlrichs, R. *Phys. Chem. Chem. Phys.* **2005**, *7*, 3297.
(21) Cao, X.; Dolg, M. *J. Mol. Struct. THEOCHEM* **2004**, *673*, 203.
(22) Küchle, W.; Dolg, M.; Stoll, H.; Preuss, H. *J. Chem. Phys.* **1994**, *100*, 7535.
(23) Hashem, E.; Swinburne, A. N.; Schulzke, C.; Evans, R. C.; Platts, J. A.; Kerridge, A.; Natrajan, L. S.; Baker, R. J. *RSC Adv.* **2013**, *3*, 4350.
(24) Woodall, S. D.; Swinburne, A. N.; Lal Banik, N.; Kerridge, A.; Di Pietro, P.; Adam, C.; Kaden, P.; Natrajan, L. S. *Chem. Commun.* **2015**, *51*, 5402.
(25) Pantazis, D. A.; Neese, F. *J. Chem. Theory Comput.* **2011**, *7*, 677.
(26) Bader, R. F. W. *Atoms in Molecules: A Quantum Theory*; Oxford University Press: Oxford, **1990**.
(27) AIMALL (Version 14.11.23), Keith, T. A., TK Gristmall Software, **2014**, Overl. Park, KS, USA
(28) Maneeprakorn, W.; Nguyen, C. Q.; Malik, M. A.; O'Brien, P.; Raftery, J. *Dalton Trans.* **2009**, 2103.
(29) Li, K.; Xue, D. *J. Phys. Chem. A* **2006**, *110*, 11332.
(30) Haigh, C. W. *Polyhedron* **1995**, *14*, 2871.
(31) Ren, W.; Song, H.; Zi, G.; Walter, M. D. *Dalton Trans.* **2012**, *41*, 5965.
(32) Ren, W.; Zi, G.; Walter, M. D. *Organometallics* **2012**, *31*, 672.
(33) Smiles, D. E.; Wu, G.; Hayton, T. W. *Inorg. Chem.* **2014**, *53*, 10240.

(34) Evans, W. J.; Miller, K. A.; Ziller, J. W.; DiPasquale, A. G.; Heroux, K. J.; Rheingold, A. L. *Organometallics* **2007**, *26*, 4287.
(35) Cloke, F. G. N.; Hawkes, S. A.; Hitchcock, P. B.; Scott, P. *Organometallics* **1994**, *13*, 2895.
(36) Thomson, R. K.; Scott, B. L.; Morris, D. E.; Kiplinger, J. L. *C. R. Chimie* **2010**, *13*, 790.
(37) Villiers, C.; Thuéry, P.; Ephritikhine, M. *Eur. J. Inorg. Chem.* **2004**, *2004*, 4624.
(38) Shannon, R. D. *Acta Crystallogr., Sect. A: Found. Crystallogr.* **1976**, *32*, 751.
(39) Nguyen, C. Q.; Adeogun, A.; Afzaal, M.; Malik, M. A.; O'Brien, P. *Chem. Commun.* **2006**, 2182.
(40) Takase, M. K.; Ziller, J. W.; Evans, W. J. *Chem. Eur. J.* **2011**, *17*, 4871.
(41) Mueller, T. J.; Ziller, J. W.; Evans, W. J. *Dalton Trans.* **2010**, *39*, 6767.
(42) Evans, W. J.; Walensky, J. R.; Ziller, J. W. *Chem. Eur. J.* **2009**, *15*, 12204.
(43) Evans, W. J.; Walensky, J. R.; Furche, F.; Ziller, J. W.; DiPasquale, A. G.; Rheingold, A. L. *Inorg. Chem.* **2008**, *47*, 10169.
(44) Evans, W. J.; Davis, B. L. *Chem. Rev.* **2002**, *102*, 2119.
(45) Jensen, M. P.; Bond, A. H.; Rickert, P. G.; Nash, K. L. *J. Nucl. Sci. Technol.* **2002**, *39*, 255.
(46) Graves, C. R.; Scott, B. L.; Morris, D. E.; Kiplinger, J. L. *Organometallics* **2008**, *27*, 3335.
(47) Graves, C. R.; Schelter, E. J.; Cantat, T.; Scott, B. L.; Kiplinger, J. L. *Organometallics* **2008**, *27*, 5371.
(48) Thomson, R. K.; Graves, C. R.; Scott, B. L.; Kiplinger, J. L. *Eur. J. Inorg. Chem.* **2009**, *2009*, 1451.
(49) Evans, W. J.; Walensky, J. R.; Ziller, J. W. *Inorg. Chem.* **2010**, *49*, 1743.
(50) Graves, C. R.; Scott, B. L.; Morris, D. E.; Kiplinger, J. L. *J. Am. Chem. Soc.* **2007**, *129*, 11914.
(51) Graves, C. R.; Yang, P.; Kozimor, S. A.; Vaughn, A. E.; Clark, D. L.; Conradson, S. D.; Schelter, E. J.; Scott, B. L.; Thompson, J. D.; Hay, P. J.; Morris, D. E.; Kiplinger, J. L. *J. Am. Chem. Soc.* **2008**, *130*, 5272.
(52) Graves, C. R.; Vaughn, A. E.; Schelter, E. J.; Scott, B. L.; Thompson, J. D.; Morris, D. E.; Kiplinger, J. L. *Inorg. Chem.* **2008**, *47*, 11879.
(53) Graves, C. R.; Kiplinger, J. L. *Chem. Commun.* **2009**, 3831.
(54) Evans, W. J.; Walensky, J. R.; Ziller, J. W. *Organometallics* **2010**, *29*, 101.
(55) Montalvo, E.; Ziller, J. W.; DiPasquale, A. G.; Rheingold, A. L.; Evans, W. J. *Organometallics* **2010**, *29*, 2104.
(56) Williams, U. J.; Robinson, J. R.; Lewis, A. J.; Carroll, P. J.; Walsh, P. J.; Schelter, E. J. *Inorg. Chem.* **2014**, *53*, 27.
(57) Kosog, B.; La Pierre, H. S.; Heinemann, F. W.; Liddle, S. T.; Meyer, K. *J. Am. Chem. Soc.* **2012**, *134*, 5284.
(58) Yin, H.; Lewis, A. J.; Williams, U. J.; Carroll, P. J.; Schelter, E. J. *Chem. Sci.* **2013**, *4*, 798.
(59) Lewis, A. J.; Nakamaru-Ogiso, E.; Kikkawa, J. M.; Carroll, P. J.; Schelter, E. J. *Chem. Commun.* **2012**, *48*, 4977.
(60) King, D. M.; Tuna, F.; McInnes, E. J. L.; McMaster, J.; Lewis, W.; Blake, A. J.; Liddle, S. T. *Nat. Chem.* **2013**, *5*, 482.

(61) Lukens, W. W.; Beshouri, S. M.; Stuart, A. L.; Andersen, R. A. *Organometallics* **1999**, *18*, 1247.
(62) Evans, W. J.; Nyce, G. W.; Johnston, M. A.; Ziller, J. W. *J. Am. Chem. Soc.* **2000**, *122*, 12019.
(63) Lukens, W. W.; Beshouri, S. M.; Blosch, L. L.; Stuart, A. L.; Andersen, R. A. *Organometallics* **1999**, *18*, 1235.
(64) Diaconescu, P. L.; Cummins, C. C. *J. Am. Chem. Soc.* **2002**, *124*, 7660.
(65) Evans, W. J.; Kozimor, S. A.; Ziller, J. W.; Fagin, A. A.; Bochkarev, M. N. *Inorg. Chem.* **2005**, *44*, 3993.
(66) Kerridge, A. *Dalton Trans.* **2013**, *42*, 16428.
(67) Kerridge, A. *RSC Adv.* **2014**, *4*, 12078.

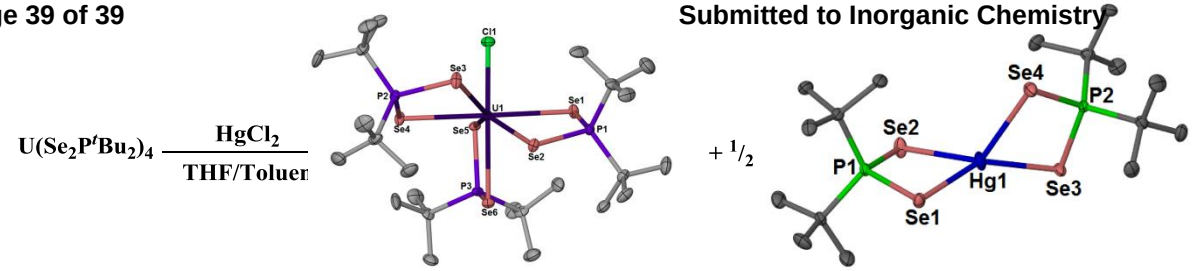

Alkyl-substituted dithio- and diselenophosphinate complexes have been synthesized and their molecular and electronic structure examined using spectroscopic techniques, X-ray crystallography, and DFT calculations. Additionally, reactivity has been observed in which late transition metal salts can be used to displace one dithio- or diselenophosphinate ligand in U(IV) complexes.